INFORMATION TO USERS

The most advanced technology has been used to photograph and reproduce this manuscript from the microfilm master. UMI films the text directly from the original or copy submitted. Thus, some thesis and dissertation copies are in typewriter face, while others may be from any type of computer printer.

The quality of this reproduction is dependent upon the quality of the copy submitted. Broken or indistinct print, colored or poor quality illustrations and photographs, print bleedthrough, substandard margins, and improper alignment can adversely affect reproduction.

In the unlikely event that the author did not send UMI a complete manuscript and there are missing pages, these will be noted. Also, if unauthorized copyright material had to be removed, a note will indicate the deletion.

Oversize materials (e.g., maps, drawings, charts) are reproduced by sectioning the original, beginning at the upper left-hand corner and continuing from left to right in equal sections with small overlaps. Each original is also photographed in one exposure and is included in reduced form at the back of the book. These are also available as one exposure on a standard 35mm slide or as a 17" x 23" black and white photographic print for an additional charge.

Photographs included in the original manuscript have been reproduced xerographically in this copy. Higher quality 6" x 9" black and white photographic prints are available for any photographs or illustrations appearing in this copy for an additional charge. Contact UMI directly to order.

U·M·I

University Microfilms International
A Bell & Howell Information Company
300 North Zeeb Road, Ann Arbor, MI 48106-1346 USA
313/761-4700 800/521-0600

Order Number 1337494

A model radiative transfer problem

Zhang, Hongbin, M.S.

The University of Arizona, 1989

U·M·I
300 N. Zeeb Rd.
Ann Arbor, MI 48106

A MODEL RADIATIVE TRANSFER PROBLEM

by

Hongbin Zhang

A Thesis Submitted to the Faculty of the

DEPARTMENT OF NUCLEAR AND ENERGY ENGINEERING

In Partial Fulfillment of the Requirements
For the Degree of

MASTER OF SCIENCE
WITH A MAJOR IN NUCLEAR ENGINEERING

In the Graduate College

THE UNIVERSITY OF ARIZONA

1989

STATEMENT BY THE AUTHOR

This thesis has been submitted in partial fulfillment of requirements for an advanced degree at the University of Arizona and is deposited in the University Library to be made available to borrowers under rules of the Library.

Brief quotations from this dissertation are allowable without special permission, provided that accurate acknowledgment of source is made. Requests for permission for extended quotation from or reproduction of this manuscript in whole or in part may be granted by the head of the major department or the Dean of the Graduate College when in his or her judgement the proposed use of the material is in the interests of scholarship. In all other instances, however, permission must be obtained from the author.

SIGNED: Hongbin Zhang

APPROVAL BY THESIS DIRECTOR

This thesis has been approved on the date shown below:

Barry Ganapol — 5/31/89

B. D. Ganapol
Professor of Nuclear and
Energy Engineering

Date

To my mother and father

ACKNOWLEDGMENTS

The author would like to express his a very personal appreciation to Dr. Barry Ganapol without whom this work would not have been possible. I would also like to acknowledge the given and much appreciated great support afforded me by Dr. Robert L. Seale and the entire Department of Nuclear and Energy Engineering at the University of Arizona.

Finally, I would like to express my sinsere gratitude to my good friends for their always present support.

TABLE OF CONTENTS

LIST OF TABLES

LIST OF FIGURES

ABSTRACT

The analytical solution to a model time-dependent continuous lethargy photon transport equation is evaluated numerically to obtain a benchmark solution using the Laplace transforms coupled with the multiple collision expansion method. The benchmark solution is then used to check the accuaracy of the multigroup approximation. Excellent agreement between continuous lethargy benchmarks and multigroup approximation is obtained.

CHAPTER 1.
INTRODUCTION

The theory of photon transport in matter, traditionally called "radiative transfer", has a great deal in common with neutron transport theory. Both theories are essentially statistical descriptions of particles transport that undergo repeated random changes in their position, energy, and direction of propagation as they travell in a medium. Since both theories ordinarily neglect interactions between the migrating particles, the starting point is the linear Boltzmann equation describing particle motion resulting from scattering and absorption interaction. Accordingly, many of the techniques that have been developed for neutron transport theory can also be applied to photon transport theory apart from trivial differences in notation and nomenclature.

This research considers benchmark solutions to the time and energy dependent radiative transport equation in an idealized one-dimensional infinite plane geometry. We are concerned only with the treatment of the equation of radiative transfer for a grey medium[1] with isotropic scattering for the purpose of presenting an analytical solution for the case where photons are emitted from a plane isotropic monoenergetic pulsed source into an infinite homogeneous plane medium. The problem chosen is an idealized model of real physical phenomena which is to be

used as a standard. Only the radiation field will be considered here. The temperature therefore will be assumed constant and unaffected by the radiation field. This problem is one of the most fundemental transport problems having application, for example, in the analysis of pulsed gamma ray experiments and numerical methods development.

Time-dependent transport problems have been studied intensively since the inception of transport theory. Even for the simplied infinite-medium problem, the time-dependent equation has required some intricate and laborious mathematical manipulation. By applying the singular eigenfunction expansion method, Case[2,3] solved the equation for a monoenergetic initial-value Green's Function (GF) problem analytically, however, leaving solutions in a non-transparent form which was not easy to implement to obtain an accurate numerical evaluation. The classical integral transform method has been one of the most obvious ways to solve the infinite medium initial value GF problem. Papmehl[4] obtained a time-dependent GF by Fourier transforming the transport equation in both the time and space coordinates. Boffi[5] sought the density arising from an isotropic, pulsed plane source by Fourier transforming the transport equation with respect to the spatial coordinate, but Laplace transforming with respect to time. By inverting the Fourier transform first and then performing the Laplace inversion, Boffi obtained expressions[5] for the density in certain asymptotic regimes after much manipulation. More recently, by means of Fourier transforming the space coordinate and Laplace transforming the time dependence, however, Palmeri[6,7] could explicitly carry out the double integral transform inversion by performing the Laplace inversion first followed by the Fourier inversion. This lead to a closed form solution for the case of isotropic scattering. These attemps then ran into the rather formidable task of inverting the resulting

transform solution, which must be approached from a purely numerical point of view.[8]

In order to find exact numerical benchmark solutions used to test both numerical computer codes and approximate analytical solutions, Ganapol[9,10,11] used the multiple collision formalism sucessfully in providing the numerical evaluation of exact solutions to various infinite and anisotropical scattering medium time-dependent monoenergetic problems. It is his method modified for the particular radiative that will be followed here.

In this presentation, we will present some new results for the solution of a radiative transfer equation using the combination of integral transforms and the multiple collision formulation of the transport equation with time and frequency dependence. In chapter II, with both a monoenergenetic and an isotropic pulsed plane source at the center of an infinite isotropic plane geometry, photon transport is studied with the multiple collision formulation at the heart of solution. The basis of the multiple collision approach lies in the decomposition of the transport equation into component equations each representing the behavior of particles of a given collision order[12]. Through this particular decomposition, the intensity of each collision order can be expressed in a form leading to the resolution of the component equations. By summing the infinite multiple collision series, we are then able to obtain a closed form expression for the scalar intensity in some cases.[6,7] The solution studied here was derived by taking the Laplace transform with respect to time followed by a simple variable transformation. The photon frequency was logorithmly transformed into a new variable corresponding to photon lethargy u. By applying the Laplace transform to u, the resulting transport equation can be reformulated

into an infinite set of multiple collision equations. The lethargy dependence can be seperated from the time and spatial dependence specificially because of the multiple collision formulation. By the application of Laplace transform inversion to the lethargy dependent component which is multiplied by a time and spatially dependent component which has already been determined previously, we obtain the solution for the scalar intensity that holds for all space, time and frequency. The advantage of this method is a double integral transform inversion is avoided in order to carry out the solutions, since it would not be possible to do double integral transform inversion numerically with today's computers.

The main focus of this work is on the development of an accurate (three to five digit) standard or benchmark solution. No discrete approximations have been made and only numerical recursion and summation are employed. The numerical solution was generated from the evaluation of an analytical representation through standard numerical techniques with internal checks on accuarcy. This paper is devoted solely to the benchmark investigation. A physical setting to fit this model problem in reality does not exist. We present some useful numerical results based on the solutions obtained to function as a guide to code developers. The results presented here are fairly simple and straightforward, and may be of pedagogical interest to the non-expert and expert alike.

In chapter III, we will apply a discretization in lethargy that is common to virtually all deterministic computational methods, namely the multi-group approximation. We will study the solution of the multigroup intego-differential equation describing photon behavior with the space-time variation. The multigroup method proposed in this paper is based on a combined analytical-numerical approach which

was originally derived and applied to one-group neutron problems[11] and then extended to multigroup problems. In this method, the lethargies of all the photons are divided into intervals called groups. The photons within each group are lumped together and are all subject to the processes of scattering and absorption. The interactions within each group interval are described in terms of suitably averaged cross sections which are collectively known as group constants[13]. In the multigroup formulation, the multiple collision-like expansion will also be employed. By means of integral transport theory and induction, the group intensity is determined analytically. The code TEMPSGP[14], originally written to calculate the group scalar flux for neutrons, will be used to obtain group scalar intensities directly with appropriate group constants.

In chapter IV, some results of the multigroup approximation calculation and comparisons with the continuous lethargy benchmark solution are presented and discussed. Finally, Chapter V contains the conclusions of this research and suggestions for future research in this subject area.

CHAPTER 2.
CONTINUOUS FREQUENCY RADIATIVE TRANSFER

2.1 Theory

Consider the equation of radiative for a one-dimensional, isotropically scattering, gray, plane medium

$$\left[\frac{\partial}{\partial t}+\mu\frac{\partial}{\partial x}+1\right]I_B(x,\mu,\nu,t)=\frac{\omega}{2}\int_{-1}^{1}d\mu'\int_{\nu}^{\infty}d\nu' f(\nu'-\nu)I_B(x,\mu',\nu',t) + B(x,\nu,t) \tag{2.1}$$

$$I_B(x,\mu,\nu,0)=0$$

where $I_B(x,\mu,\nu,t)$ is the angular radiation intensity, x is measured in units of the total mean-free-path (by replacing x by $x\sigma_t$) and t is mean-free-time (by replacing t by $t\sigma_t c$). ν is the frequency of photon, ω is the mean number of photons produced per collision or the number of secondary photon per collision (single scattering albedo). $f(\nu'-\nu)$ is the scattering kernel describing the probability of scattering from wavelength ν' to $d\nu$ about ν with only down scattering case considered. This scattering kernel is chosen based on Compton scattering where photons scatter from free electrons at rest. Compton scattering is the most important form of scattering

process in radiation hydradynamic problems. The scattering kernel for Compton scattering is given by Klein-Nishina formula[15]

$$\sigma_s(\nu \to \nu', \xi) = N\frac{r_0^2}{2}\frac{1+\xi^2}{[1+\gamma(1-\xi)]^2}\left[1+\frac{\gamma^2(1-\xi)^2}{(1+\xi^2)[1+\gamma(1-\xi)]}\right]\cdot \\ \cdot \delta(\nu' - \frac{\nu}{1+\gamma(1-\xi)}) \tag{2.2}$$

where $\xi = \bar{\Omega}\cdot\bar{\Omega}'$, N is the electron density and r_0 is the classical electron radius. γ is a dimensionless frequency, $\gamma = h\nu/m_0c^2$. We see from the argument of the delta function in this formula that the final energy is always less than the initial energy[15]. Note that Eq. (2.1) indicates that the photon frequency redistribution is of a particular form, isotropic and dependent on $\nu - \nu'$ only. This special scattering kernel suggests the possibility of using the convolution theorem and considered for this reason. $B(x,\nu,t)$ is the source of photons resulting from a blackbody emmision, thus $B(x,\nu,t)$ is Planck function

$$B(x,\nu,t) = \frac{2h\nu^3}{c_0^2 exp(h\nu/kT) - 1} \tag{2.3}$$

where h and k are the universal Planck and Boltzmann constants, respectively, c_0 is the speed of light in a vacuum, and T is the absolute temperature of the blackbody (K)[16]. Here T is considered to be constant through the medium.

This equation can be solved by means of the initial-value infinite-medium Green's function

$$I_B(x,\mu,\nu,t) = \int_{-\infty}^{\infty} dx_0 \int_0^t dt_0 \int_{-1}^{1} d\mu_0 \int_0^{\infty} d\nu_0 B(x_0,\nu_0,t_0)\cdot \\ \cdot I(x,\mu,\nu,t;x_0,\mu_0,\nu_0,t_0), \tag{2.4}$$

where $I(x,\mu,\nu,t;x_0,\mu_0,\nu_0,t_0)$ is the Green's function satisfying

$$\left[\frac{\partial}{\partial t}+\mu\frac{\partial}{\partial x}+1\right]I(x,\mu,\nu,t;x_0,\mu_0,\nu_0,t_0)=$$
$$\frac{\omega}{2}\int_{-1}^{1}d\mu'\int_{\nu}^{\infty}d\nu' f(\nu-\nu')I(x,\mu',u',t;x_0,\mu_0,\nu_0,t_0)$$
$$+\delta(x-x_0)\delta(\nu-\nu_0)\delta(\mu-\mu_0)\delta(t-t_0) \tag{2.5}$$

$$\lim_{|x|\to\infty} I(x,\mu,\nu,t;x_0,\mu_0,\nu_0,t_0)=0$$

$$I(x,\mu,\nu,t;x_0,\mu_0,\nu_0,t_0)=0, \qquad t<0.$$

Applying translational invariance, we have

$$I(x-x_0,\mu,\nu,t-t_0;\mu_0,\nu_0)=I(x,\mu,\nu,t;0,\mu_0,\nu_0,0), \tag{2.6}$$

which obeys

$$\left[\frac{\partial}{\partial t}+\mu\frac{\partial}{\partial x}+1\right]I(x,\mu,\nu,t)=\frac{\omega}{2}\int_{-1}^{1}d\mu'\int_{\nu}^{\infty}d\nu' f(\nu'-\nu)I(x,\mu',\nu',t)$$
$$+\delta(x)\delta(\nu-\nu_0)\delta(\mu-\mu_0)\delta(t)$$

$$\lim_{|x|\to\infty} I(x,\mu,\nu,t)=0 \tag{2.7}$$

where x replaces $x-x_0$ and t replaces $t-t_0$, μ_0 and ν_0 in $I(x,\mu,\nu,t;\mu_0,\nu_o)$ are suppressed for ease of notation. We will now solve the Green's function analytically.

When the Laplace transform with respect to t,

$$\bar{I}(x,\mu,\nu,s)=\int_0^{\infty}e^{-st}I(x,\mu,\nu,t)dt, \tag{2.8}$$

is applied to equation (2.7), we obtain the following equation for $\bar{I}(x,\mu,\nu,t)$

$$\left[s+\mu\frac{\partial}{\partial x}+1\right]\bar{I}(x,\mu,\nu,s)=\frac{\omega}{2}\int_{-1}^{1}d\mu'\int_{\nu}^{\infty}d\nu' f(\nu-\nu')\bar{I}(x,\mu',\nu',s)$$
$$+\delta(x)\delta(\nu-\nu_0)\delta(\mu-\mu_0)$$

$$\lim_{|x|\to\infty} \bar{I}(x,\mu,\nu,s) = 0. \tag{2.9}$$

A new variable u is defined as photon lethargy which is identical to the lethargy used in neutron transport theory

$$u = \ln \frac{\nu_0}{\nu}. \tag{2.10a}$$

Thus

$$du = -\frac{d\nu}{\nu} \tag{2.10b}$$

and

$$\delta(\nu - \nu_0) = \frac{\delta(u)}{\nu} \tag{2.10c}$$

$$\bar{I}(x,\mu,\nu,s) = \frac{\bar{I}(x,\mu,u,s)}{\nu} \tag{2.10d}$$

$$f(\nu' - \nu) = \frac{f(u-u')}{\nu}. \tag{2.10e}$$

Equation (2.9) then becomes

$$\left[s + \mu\frac{\partial}{\partial x} + 1\right]\bar{I}(x,\mu,u,s) = \frac{\omega}{2}\int_{-1}^{1} d\mu' \int_0^u du' f(u-u')\bar{I}(x,\mu',u',s) + \delta(x)\delta(u)\delta(\mu-\mu_0). \tag{2.11}$$

Then by taking the Laplace transform with respect to u of equation (2.11)

$$\bar{\bar{I}}(x,\mu,p,s) = \int_0^\infty e^{-pu}\bar{I}(x,\mu,u,s)du \tag{2.12}$$

and using the convolution theorem, we find

$$[s + \mu\frac{\partial}{\partial x} + 1]\bar{\bar{I}}(x,\mu,p,s) = \omega\frac{\bar{f}(p)}{2}\int_{-1}^{1} d\mu'\bar{\bar{I}}(x,\mu',p,s) + \delta(x)\delta(\mu-\mu_0) \tag{2.13}$$

$$\lim_{|x|\to\infty} \bar{\bar{I}}(x,\mu,p,s) = 0.$$

$\bar{f}(p)$ is the Laplace transform of $f(u)$, $\bar{f}(p) = \int_0^\infty e^{-pu} f(u)$. Since Eq. (2.13) is essentially a one-group transport equation, $\bar{\bar{I}}(x, \mu, p, s)$ can be recast into the following convergent multiple collision series[11]:

$$\bar{\bar{I}}(x, \mu, p, s) = \sum_{n=0}^{\infty} [\bar{f}(p)]^n \bar{\bar{\psi}}_n(x, \mu, p, s). \tag{2.14}$$

When Eq. (2.14) is introduced into equation (2.11), we obtain the set of multiple collision equations:

for n=0 (uncollided)

$$\left[s + \mu \frac{\partial}{\partial x} + 1 \right] \bar{\bar{\psi}}_0(x, \mu, p, s) = \delta(x)\delta(\mu - \mu_0) \tag{2.15a}$$

and for $n \geq 1$ (collided)

$$\left[s + \mu \frac{\partial}{\partial x} + 1 \right] \bar{\bar{\psi}}_n(x, \mu, p, s) = \frac{\omega}{2} \int_{-1}^{1} d\mu' \bar{\bar{\psi}}_{n-1}(x, \mu, p, s) \tag{2.15b}$$

$$\lim_{|x| \to \infty} \bar{\bar{\psi}}_n(x, \mu, p, s) = 0.$$

The solution to equation (2.15a) is found to be;

$$\bar{\bar{\psi}}_0(x, \mu, p, s) = \frac{1}{\mu} exp \left[-\frac{(1+s)x}{\mu} \right] \delta(\mu - \mu_0). \tag{2.16}$$

This result shows that the uncollided intensity is actually independent of p. Since the collided photons result from the uncollided photons, the uncollided intensity behavior is inherited by collided intensity; consequently, $\bar{\bar{\psi}}_n(x, \mu, p, s)$ will also be independent of p. By performing the Laplace transform inversion in equation (2.16), we obtain the usual uncollided intensity

$$\psi_0(x, \mu, t) = \frac{e^{-t}}{t} \delta(\mu - \eta)\delta(\mu - \mu_0), \tag{2.17}$$

where $\eta = x/t$. This quantity represents the characteristic variable for particle motion in an infinite medium[11]. Equation (2.15b) can therefore be inverted to give the one-group transport equation for the nth collided decomposed intensity which is identical to the neutron transport case

$$\left[\frac{\partial}{\partial t} + \mu\frac{\partial}{\partial x} + 1\right]\psi_n(x,\mu,t) = \frac{\omega}{2}\int_{-1}^{1} d\mu'\psi_{n-1}(x,\mu',t) \tag{2.18}$$

$$\lim_{|x|\to\infty} \psi_n(x,\mu,t) = 0,$$

$$\psi_n(x,\mu,t) = 0 \qquad t < 0.$$

Equation (2.18) has been numerically evaluated using the code TEMPS[11] in order to get the individual collisional components $\psi_n(x,t)$ of the scalar intensity. Finally, by recombing the solutions for spatial, time and lethargy dependence of multiple collision formulation series, the scalar intensity turns out to be of the following form (with an integral transform inversion remaining):

$$I(x,u,t) = \psi_0(x,t)\delta(u) + \sum_{n=1}^{\infty} f_n(u)\psi_n(x,t), \tag{2.19}$$

where $f_n(u) = \mathcal{L}_u^{-1}[\bar{f}(p)]^n$. The second term on the right side of equation (2.19) is the contribution of collided photon intensity. $\psi_n(x,t)$ (for $n \geq 1$) is the collided intensity of order n for the one-group equation. $f_n(u)$ is the function required to obtain the lethargy dependent intensity. The scalar intensity is then processed numerically in order to produce meaningful graphical representations which are discussed both with respect to physical and computational grounds in section (2.3).

2.2 Numerical Evaluation

The evaluation of the lethargy dependent scalar intensity given by Eq. (2.19) involves the following numerical approximations:

a). the evaluation of $f_n(u)$

b). the evaluation of $\psi_n(x,t)$.

In the remainder of the work, we investigate a simple case where the Laplace inversion can be performed analytically. Let

$$f(u) = exp(-\alpha u) \tag{2.20}$$

therefore the energy variation turns out simply to be

$$f_n(u) = \pounds_u^{-1}[\bar{f}(p)]^n \tag{2.21a}$$

that is

$$f_n(u) = \frac{e^{-\alpha u}}{(n-1)!}u^{n-1}. \tag{2.21b}$$

It is noticed that the $f_n(u)$ can be obtained numerically for general scattering kernel. For simplicity, the Eq. (2.20) is chosen.

$\psi_n(x,t)$ has been previously determined numerically in code TEMPS[11] which was originally written for neutron transport. For completeness, the numerical evaluation of $\psi_n(x,t)$ will be described briefly. The code TEMPS[11] has been developed to provide accurate time-dependent fluxes for a variety of anisotropically scattering, one-dimensional, infinite-medium one-group problems. The general one-group neutron transport equation in plane infinite geometry with a pulsed source at x=0 is

$$\left[\frac{\partial}{\partial t} + \mu\frac{\partial}{\partial x} + 1\right]\phi(x,\mu,t) = c\int_{-1}^{1} d\mu' g(\mu' \to \mu)\phi(x,\mu',t) + Q(\mu)\delta(x)\delta(t), \tag{2.22}$$

where $\phi(x,\mu,t)$ is the angular flux, c is the number of secondaries and $g(\mu' \rightarrow \mu)$ is the anisotropic scattering kernel. The scalar flux can be expanded in the following convergent multiple collision series:

$$\phi(x,t) = \sum_{n=0}^{\infty} \psi_n(x,t) \tag{2.23}$$

where

$$\psi_n(x,t) = \frac{e^{-t}}{t}\frac{(ct)^n}{n!}\psi_n(\eta)\theta(1-|\eta|) \tag{2.24}$$

$\theta(u)$ is the Heaviside step function. The reduced collided scalar flux $\psi_n(\eta)$ is nonzero for $|\eta| \leq 1$; therefore, it can be expressed as the following Legendre Polynomial expansion in the variable η:

$$\psi_n(\eta) = \sum_{k=0}^{\infty} \frac{2k+1}{2} f_{n,k}^0 P_k(\eta), \qquad n \geq n_s \tag{2.25}$$

where

$$f_{n,k}^0 = \int_{-1}^{1} d\eta P_k(\eta)\psi_n(\eta). \tag{2.26}$$

The the scalar flux becomes

$$\phi(x,t) = \frac{e^{-t}}{t}\sum_{n=0}^{n_s-1}\frac{(ct)^n}{n!}\psi_n(\eta) + \sum_{k=0}^{\infty}\frac{2k+1}{2}f_k(t)P_k(\eta) \tag{2.27}$$

where

$$f_k(t) = \frac{e^{-t}}{t}\sum_{n=n_s}^{\infty}\frac{(ct)^n}{n!}f_{n,k}^0. \tag{2.28}$$

As the result of singular nature of the source, the uncollided scalar flux and in some cases the first collided flux are also singular. Since the very slow convergence of legendre expansion near singularities, it is best to remove these components from the expansion. In Eq. (2.27), uncollided and in some instances the first collided fluxes can be obtained analytically ($n < n_s$). A recursion algebraic relation has

been found to determine the expansion coefficient $f^0_{n,k}$ after $g(\mu' \rightarrow \mu)$ has been expanded in terms of the truncated Legendre polynomials

$$g(\mu' \rightarrow \mu) = \sum_{l=0}^{L} \frac{2l+1}{2} \omega_l P_l(\mu) P_l(\mu') \qquad \omega_0 = 1 \tag{2.29}$$

$$f^l_{n,0} = (\omega_l)^n f^l_{0,0} \qquad f^l_{0,0} = \int_{-1}^{1} d\eta P_l(\eta) Q(\eta) \tag{2.30a}$$

$$(k+n) f^l_{n,k} = -(k-n-1) f^l_{n,k-2} + \frac{2k-1}{2l+1} \left[l f^{l-1}_{n,k-1} + (l+1) f^{l+1}_{n,k-1} \right] + n\omega_l \left[f^l_{n-1,k} - f^l_{n-1,k-2} \right] \tag{2.30b}$$

where

$$f^l_{n,k} = 0 \qquad k < 0.$$

In addition

$$f^l_{0,k} = \int_{-1}^{1} d\eta P_l(\eta) Q(\eta) \tag{2.30c}$$

which is the starting condition to determine $f^0_{n,k}$ required for evaluating the scalar flux given by equation (2.27). The numerical implementation of Eq. (2.27) requires three numerical procedures including the determination of

a) the expansion coefficients $f^0_{n,k}$ from the recursion relation (2.30)

b) multiple collision summation (over n)

c) Legendre series summation (over k).

The multiple collision component, $\psi_n(x,t)$ given by Eq. (2.24) is determined as a part of the multiple collision summation procedure. Once $\psi_n(x,t)$ has been

determined, it is multiplied by the appropriate $f_n(u) = \mathcal{L}_u^{-1}[\bar{f}(p)]^n$ providing the following approximation to $I(x,u,t)$

$$I(x,u,t) \cong \sum_{n=0}^{N} \mathcal{L}_u^{-1}[\bar{f}(p)]^n \psi_n(x,t) \tag{2.31}$$

this procedure is continued until the relative difference between the last term added and the partial sum is less than a specified tolerance.

2.3 Results and Discussion

All the results presented are for isotropic plane pulsed photon source and purely scattering medium (single albedo $\omega = 1$).

Figures 2.1a-h present the comparsion of the influence of different values of α on scalar intensity distribution in lethargy. It can be concluded from the figures that smaller values of α cause a greater photon intensity at the higher lethargies for any particular instant of time. This is true because for lower values of α, the photons have a higher probability ($f(u) = e^{-\alpha u}$) of reaching the same lethargy. More photons appear and accumulate at higher lethargy for any one collision if $\alpha < 1$. This is most evident when $\alpha = 0$, for which case the intensity increases the fastest as lethargy and time increase. Since the scattering kernel $f(u) = e^{-\alpha u}$ is normalized to $1/\alpha$, if $\alpha < 1$ the medium acts like a reproductive one. Thus for pure scattering ($\omega = 1$), when $\alpha < 1$, the system is identical to the supercritical neuton transport problem. This is the reason for the rapidly increasing intensity for small values of α with increasing time.

Figures 2.2a and 2.2b, present the comparison of the influence of three different values of α on the photon intensity distribution in time for x=1 and 4 mfp with u=1. As before for smaller values of α, the intensity increased at a given lethargy at any particular time. It was also found that the intensity when x=t initially increased very quickly as photons begin to arrive at that position. A peak then results as the intensity subsequently decreases. For example at x=1 with u=1, the uncollided photons just arrive when t=1. Once emitted, the scattered photons require time to slow down by collision and therefore do not arrive until after x=1. The intensity initially increases very quickly since many more photons are arriving than are being scattered from this position. At the peak the number of photons scattering to this position equals that scattered away. The shape of the intensity distributions in time at particular lethargies are similar at different positions, however, the magnitudes decrease at positions further away from source because the photons experience more collisions, thus sending more and more photons to higher lethargies.

Figures 2.3a-d show the intensity variation with lethargy and the spatial positions for various times and an α of one. Figures 2.3e-h are for α =0.1 and various t. The graphs show the spatial and lethargy development of the photon intensity as time increases. It is easily seen that with increasing time, the photon density appears more intense at higher lethargies. Furthermore, the distribution is shifted towards higher values of position. As before, for different values of α, the pattern development is the same. The smaller α values increase the intensity and rapidity of the lethargy development because of the higher probability of collision.

Figures 2.4a-i show the entire photon intensity distribution at particular spatial coordinates. Figures 2.4a-d are for α of 1 and 2.4e-h are for α of 0.5. The whole process of photon travelling and slowing down can be observed from these series of figures. When time is small, at a position close to the source more low lethargy photons exist because they have had fewer collisions. As time increases, the photons penetrate to and collide at further positions and the intensity gradually becomes more intense at higher lethargies. We also find that smaller α values cause more photons to reach higer lethargy levels at the same times than larger α values.

2.4 Limition of Theory

This model was built upon the assumption of no up scattering, similiar to Compton scattering. Under this assumption, it is always true that the final energy is less than the initial energy. In the case of up-scattering, like the the photons interact with moving electrons, called the inverse Compton scattering. The electrons can impart some or all of their energy to photons and increase photons' frequency. This model can not give accurate results when up scattering is present. However, in the case of photons scattering from a relativistic Maxwellian gas of free, non-degenerate, electrons. The scattering kernel is derived as

$$\sigma_s(\nu \to \nu', \xi) = \frac{N r_0^2}{2\gamma\nu} \int d\bar{v} f(v) \frac{1}{\lambda} \delta(\xi - 1 + \frac{\lambda D}{\gamma'} - \frac{\lambda D'}{\gamma}) \cdot \cdot \left[1 + [1 - \frac{(1-\xi)^2}{\lambda^2 D D'}] + \frac{\gamma\gamma'(1-\xi)^2}{\lambda^2 D D'}\right]. \quad (2.29)$$

The Legendre moments of this scattering kernel are defined in the usual way as

$$\sigma_{sn}(\nu \to \nu') = 2\pi \int_{-1}^{1} d\xi P_n(\xi) \sigma_s(\nu \to \nu', \xi). \quad (2.30)$$

Some typical results for these moments are shown in figures 2.5a-c. We could see from these figures that although the pure down scattering assumption is never true for inverse Compton scattering, it is still a very good approximation to the reality except for lower energy photons. We can conclude that the method developed in this work is applicable to high energy photons. In next section, we will test the accuaracy of multigroup algorithm.

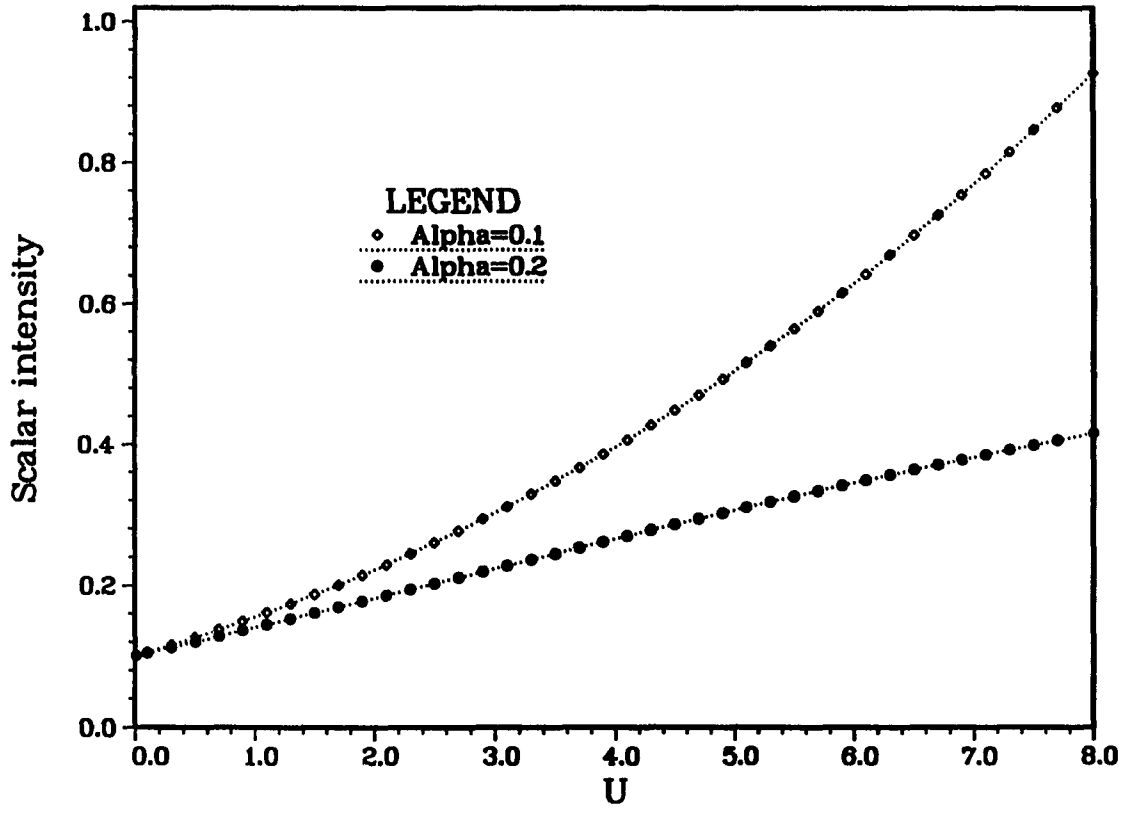

Figure 2.1a Comparison of Different Values of α at x=1 and t=1.5

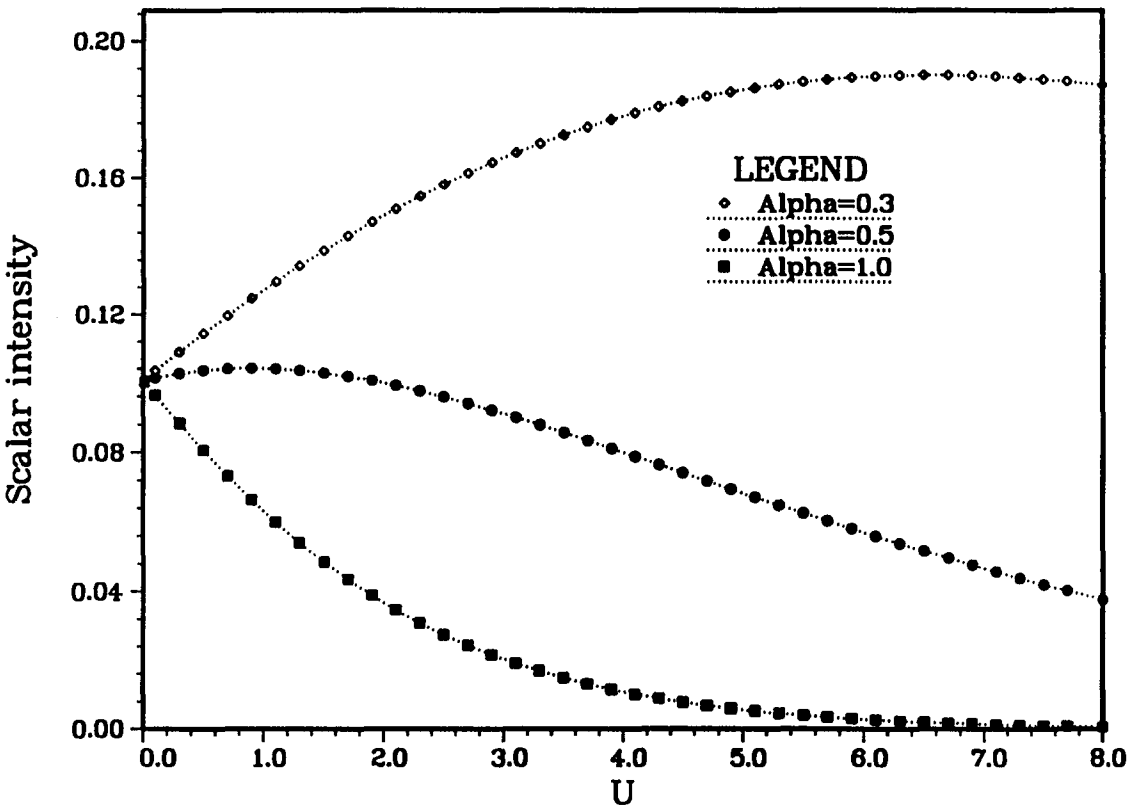

Figure 2.1b Comparison of Different Values of α at x=1 and t=1.5

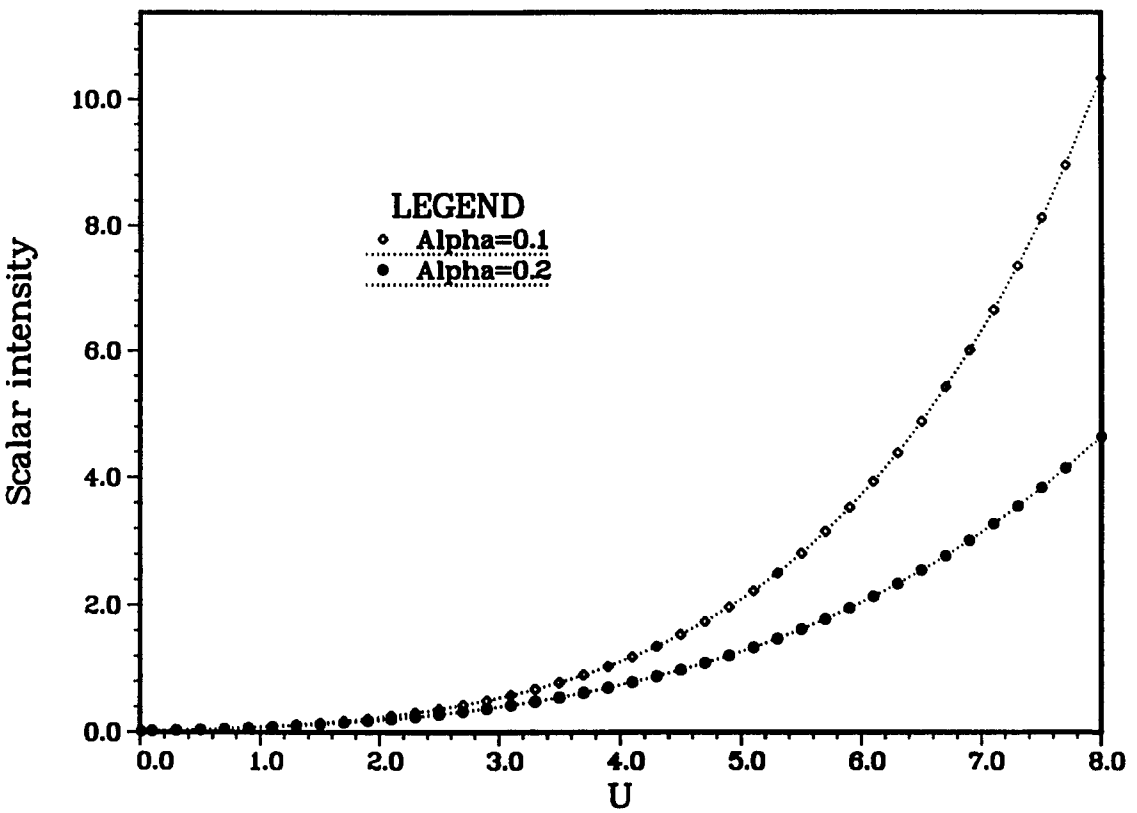

Figure 2.1c Comparison of Different Values of α at x=1 and t=3.5

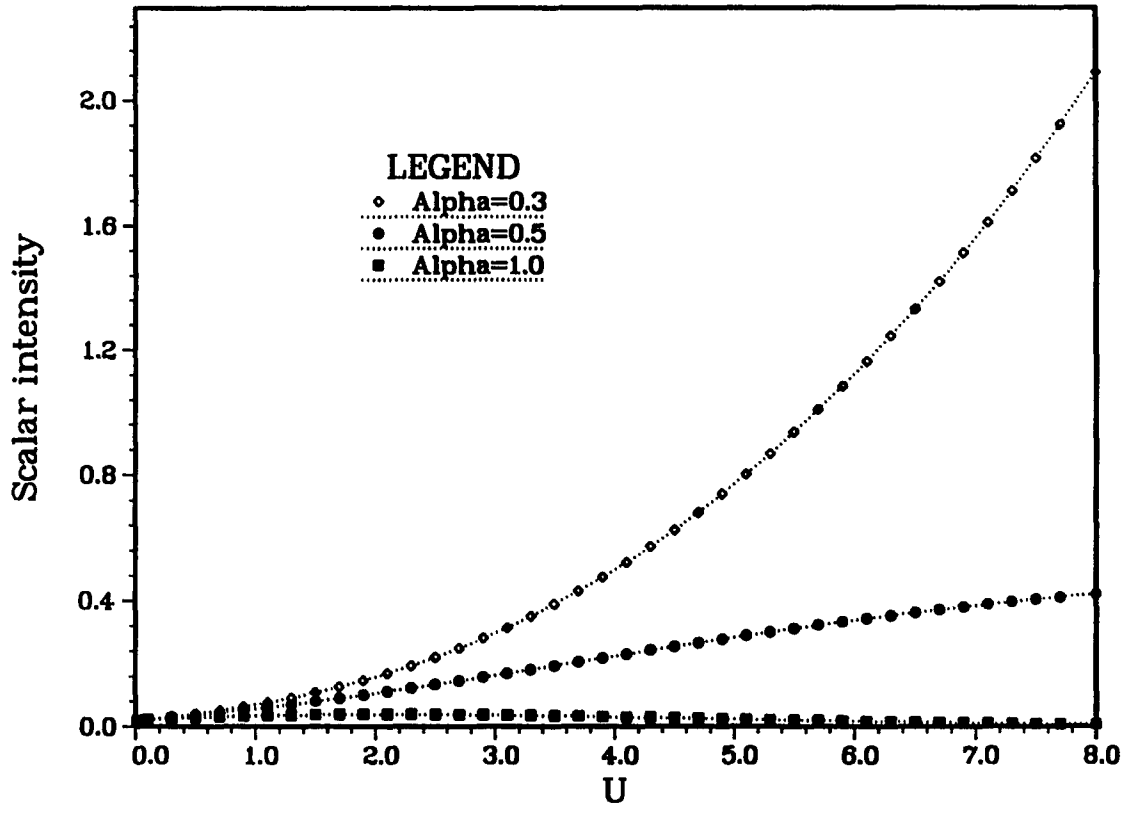

Figure 2.1d Comparison of Different Values of α at x=1 and t=3.5

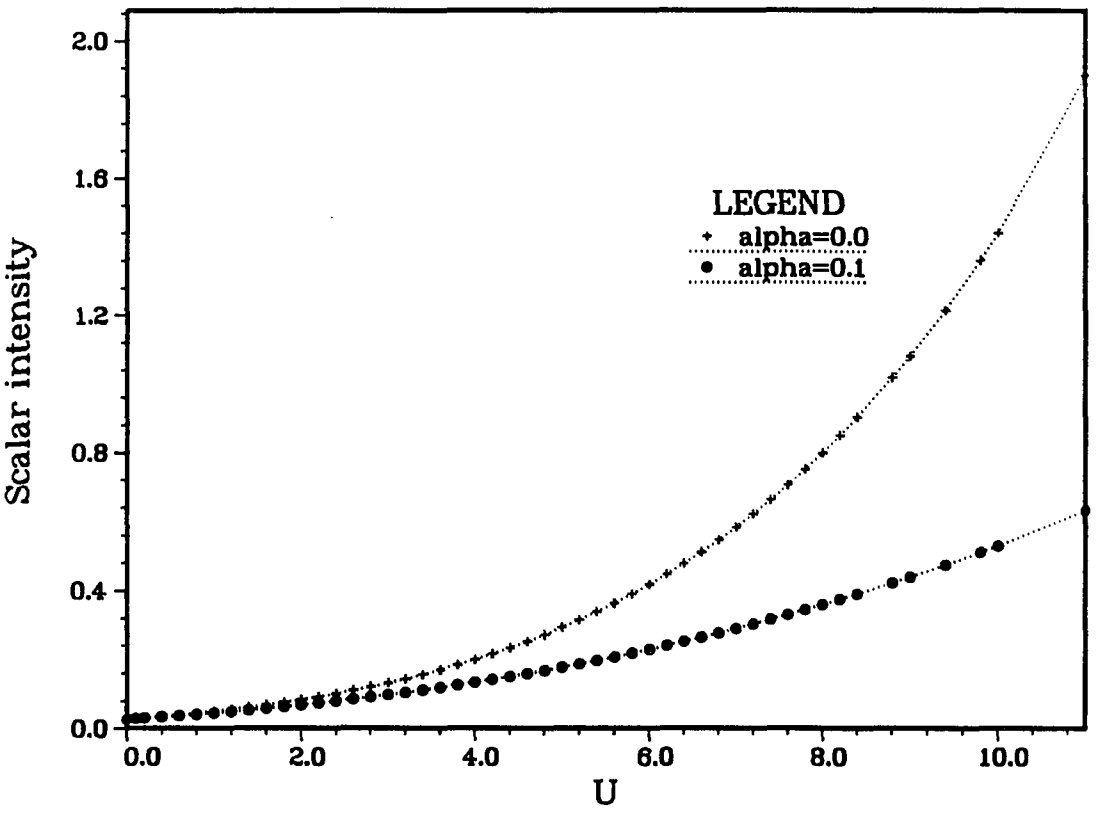

Figure 2.1e Comparison of Different Values of α at x=2 and t=2.5

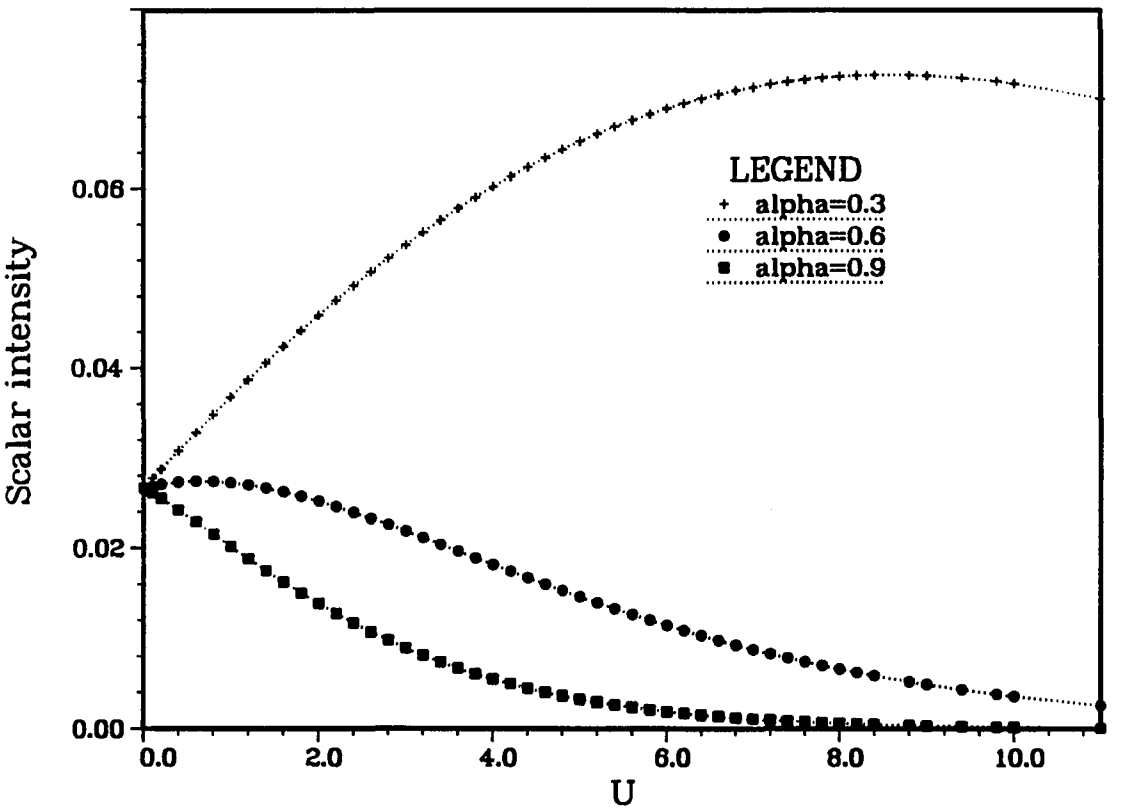

Figure 2.1f Comparison of Different Values of α at x=2 and t=2.5

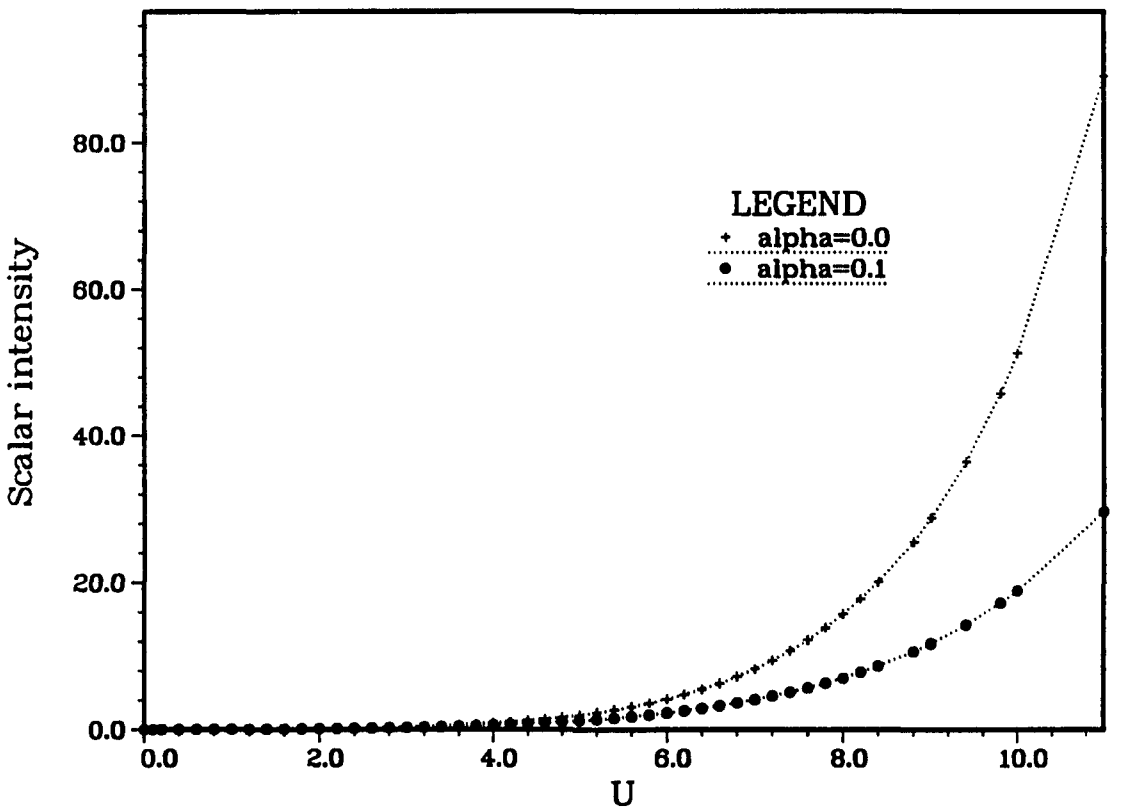

Figure 2.1g Comparison of Different Values of α at x=2 and t=4.5

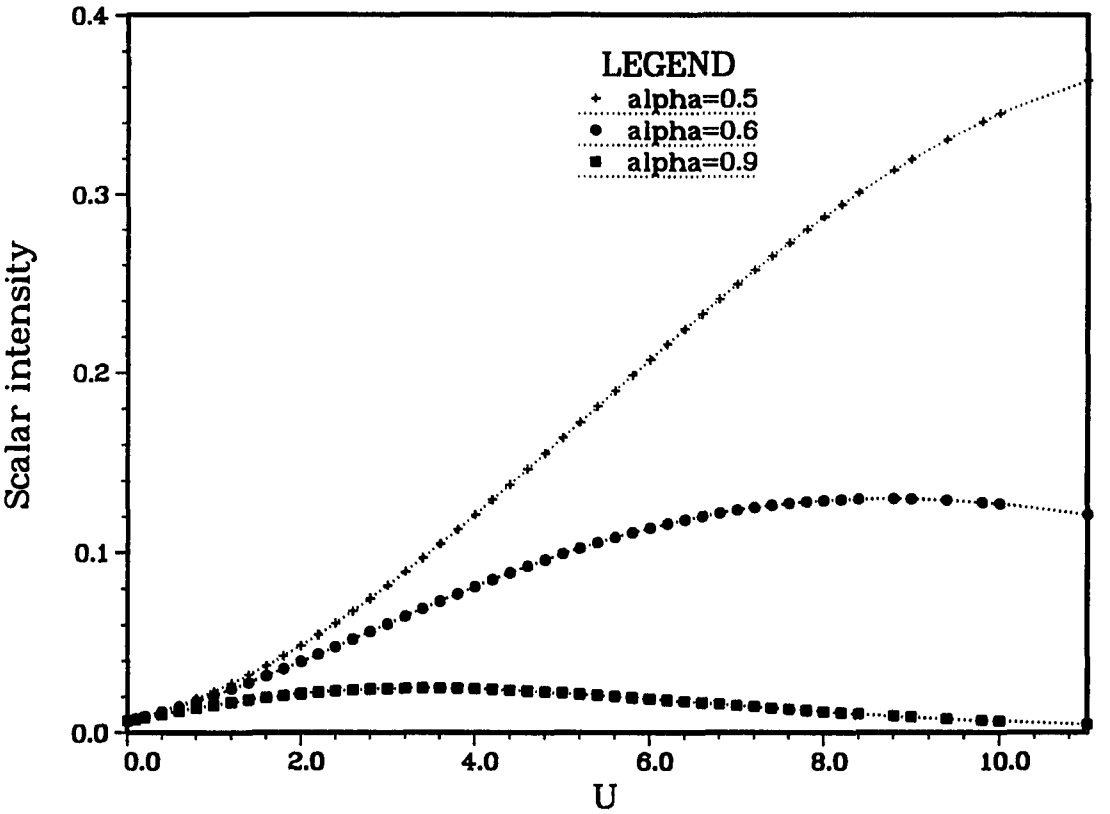

Figure 2.1h Comparison of Different Values of α at x=2 and t=4.5

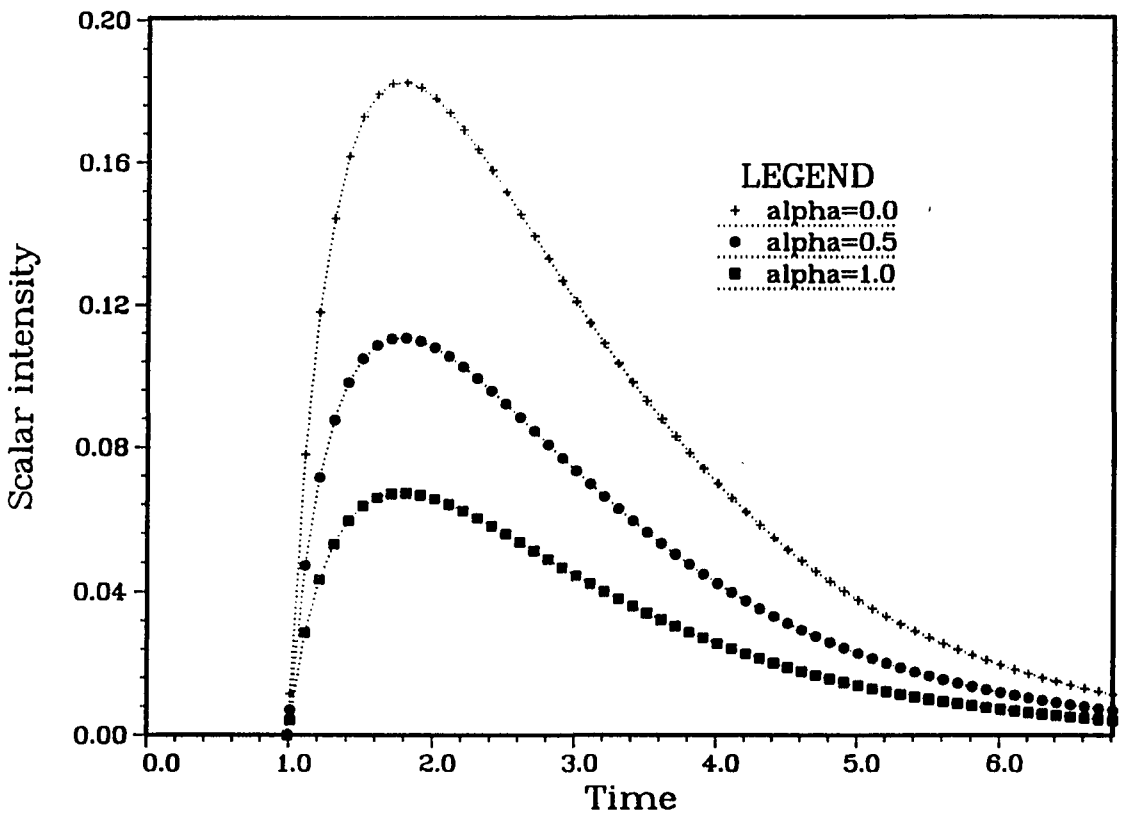

Figure 2.2a Comparison of Different Values of α at x=1 with u=1

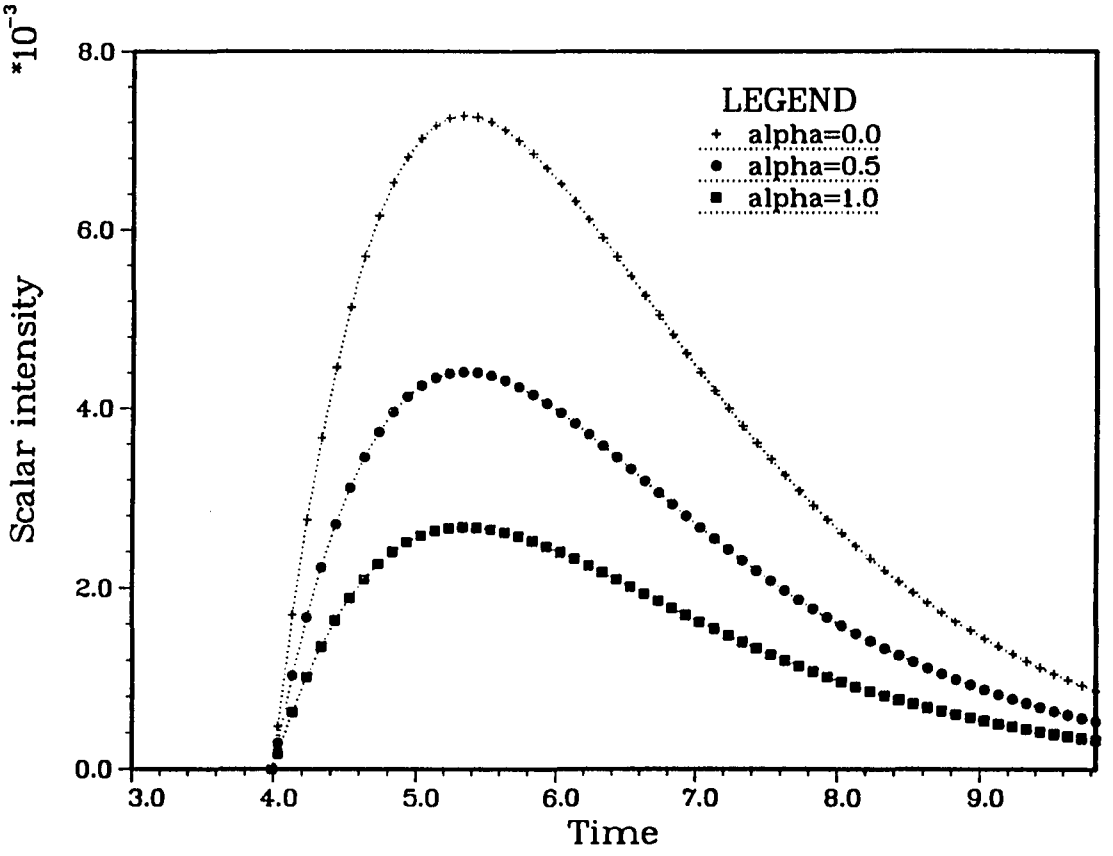

Figure 2.2b Comparison of Different Values of α at x=4 with u=1

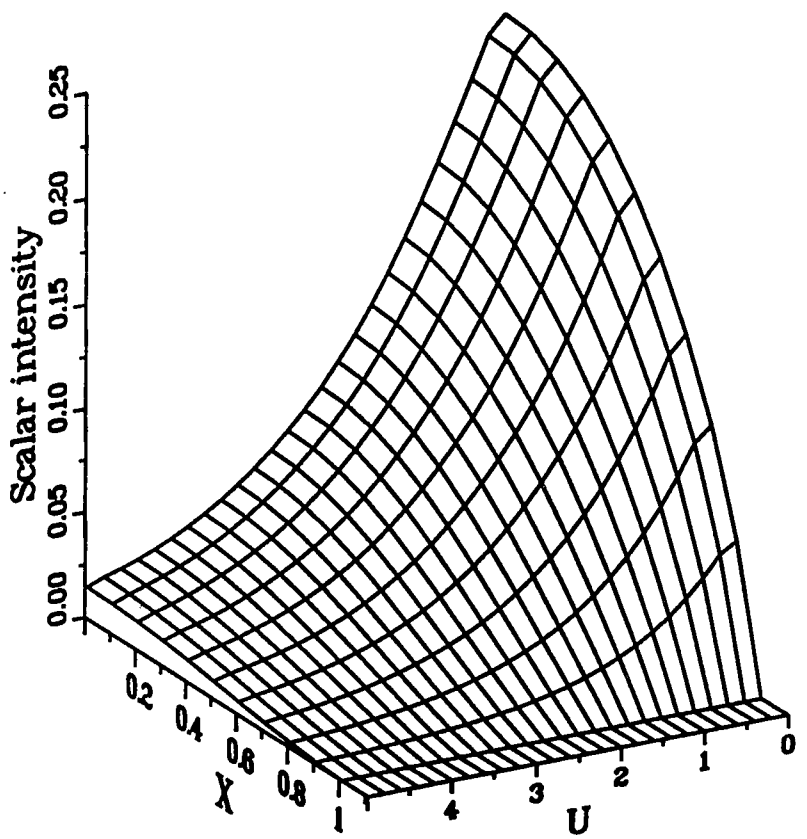

Figure 2.3a Intensity Distribution of Space and Lethargy at t=1 and α=1

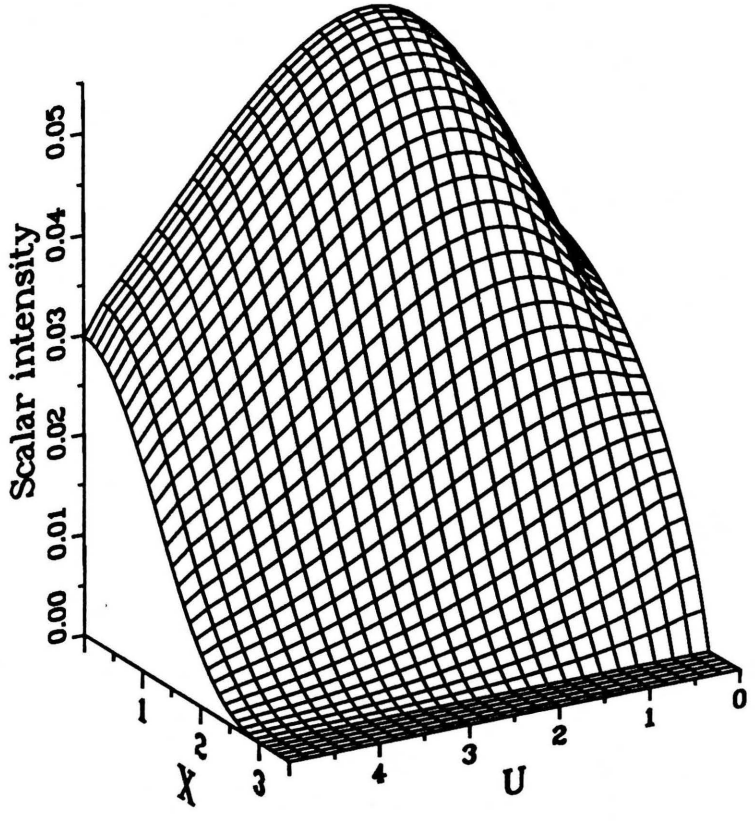

Figure 2.3b Intensity Distribution of Space and Lethargy at t=3 and α=1

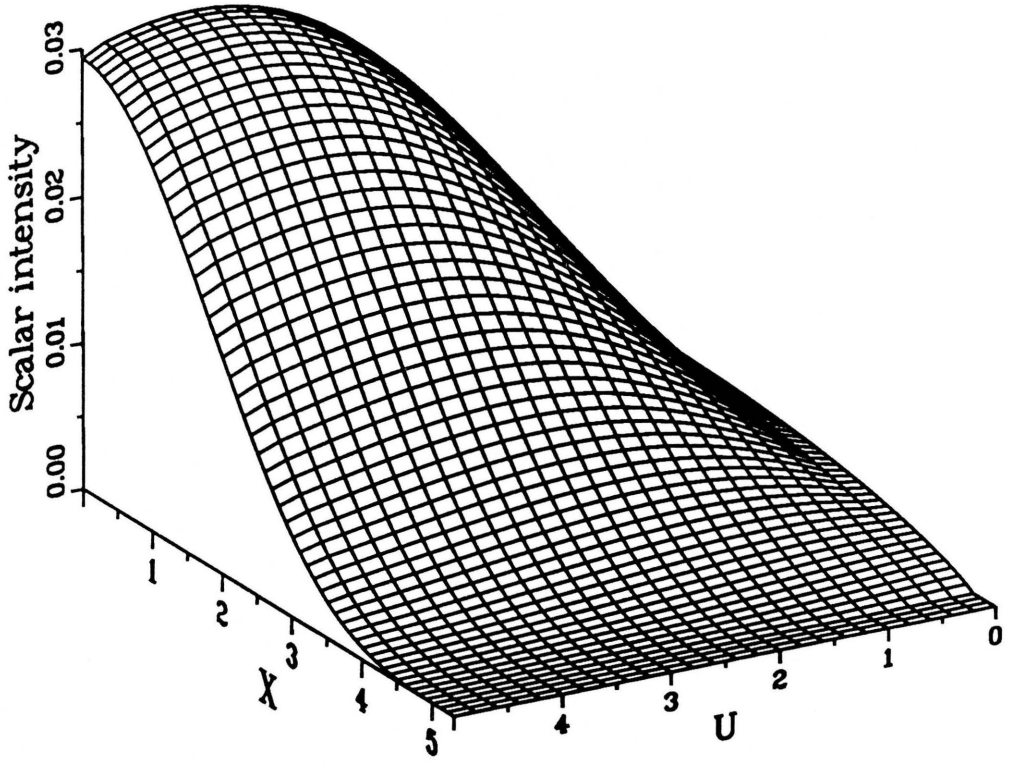

Figure 2.3c Intensity Distribution of Space and Lethargy at t=5 and α=1

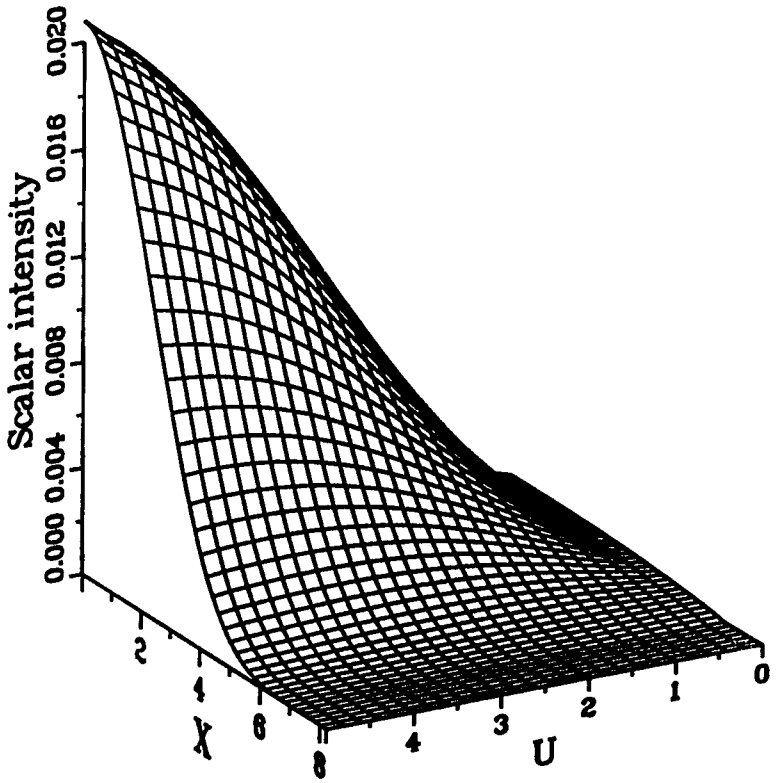

Figure 2.3d Intensity Distribution of Space and Lethargy at t=7 and α=1

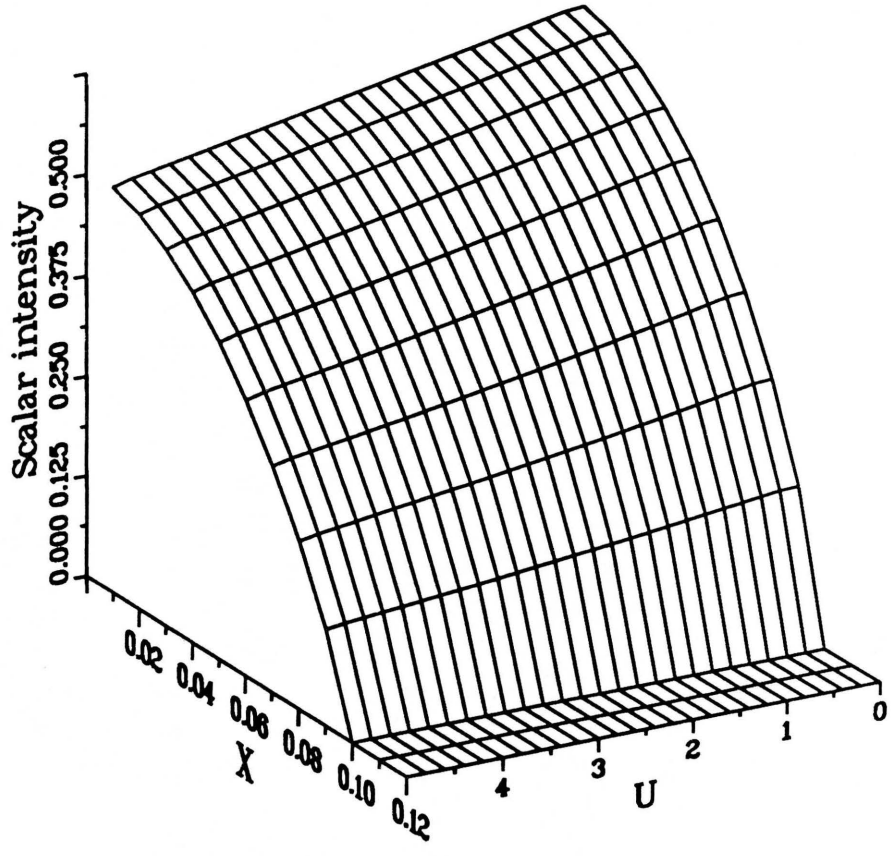

Figure 2.3e Intensity Distribution of Space and Lethargy at t=0.1 and α=0.1

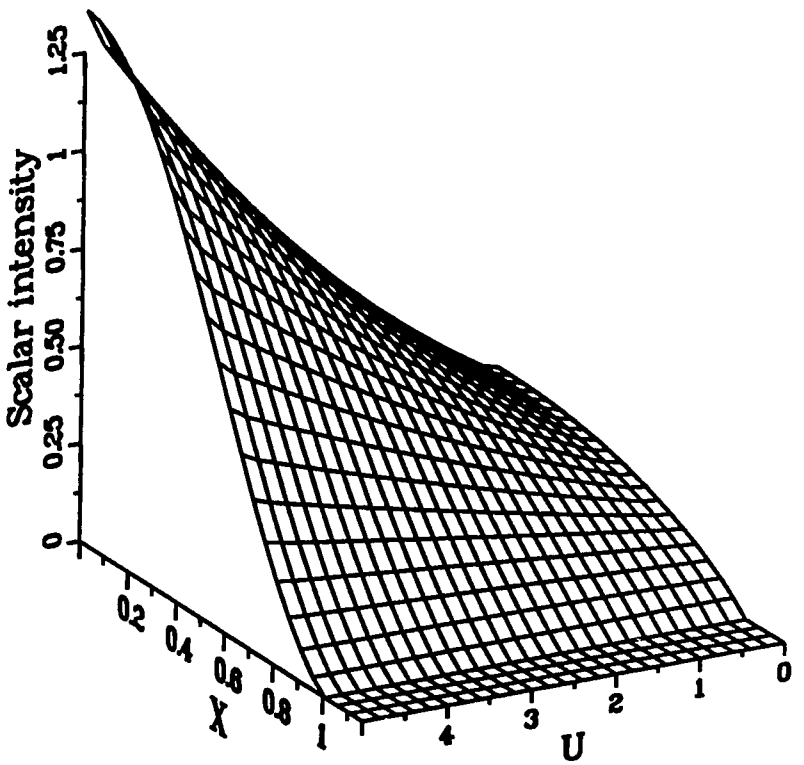

Figure 2.3f Intensity Distribution of Space and Lethargy at t=1 and α=0.1

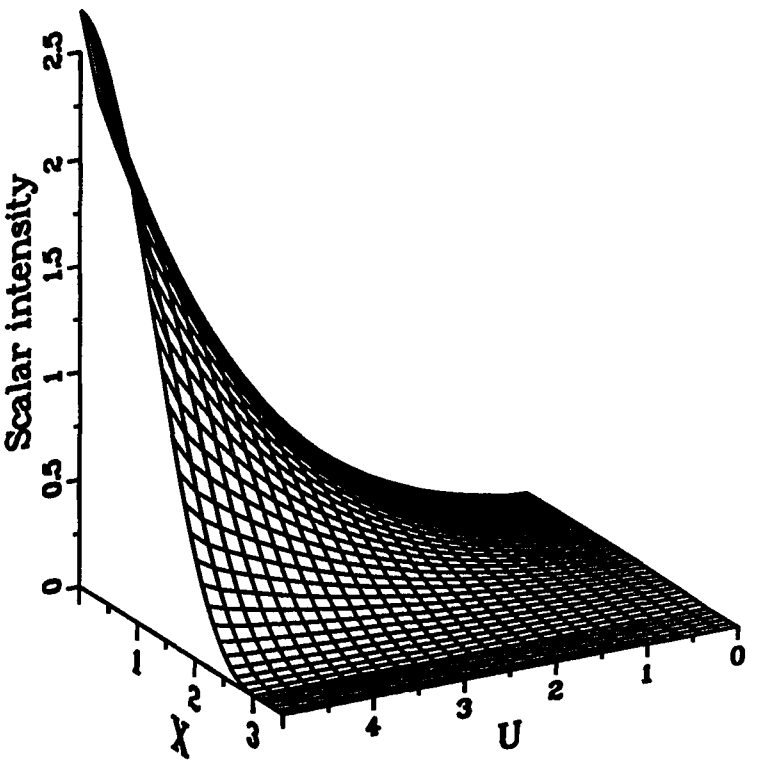

Figure 2.3g Intensity Distribution of Space and Lethargy at t=3 and α=0.1

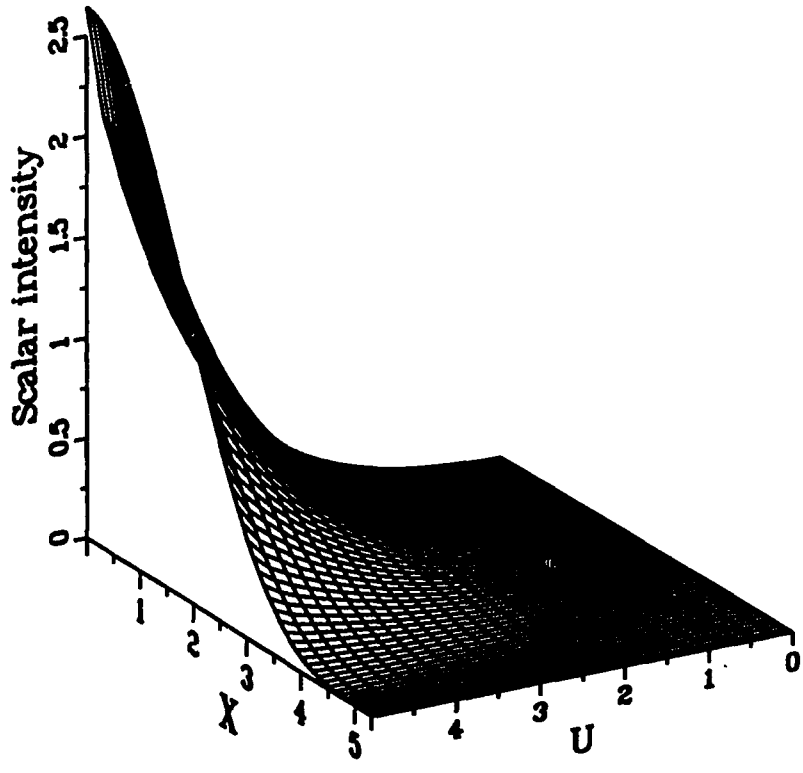

Figure 2.3h Intensity Distribution of Space and Lethargy at t=5 and α=0.1

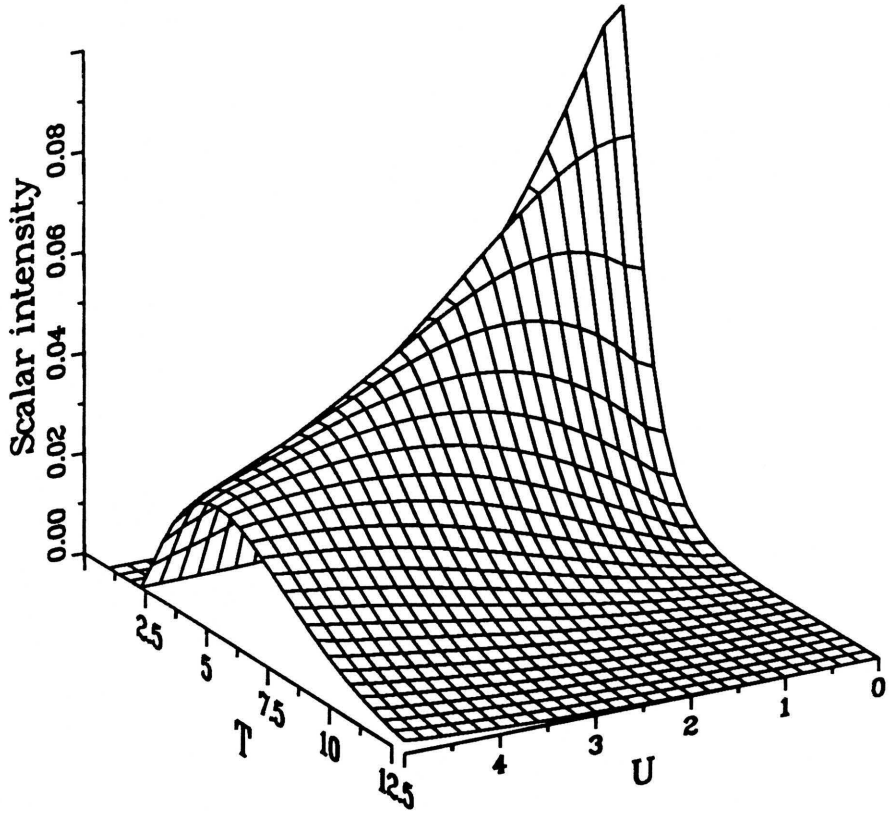

Figure 2.4a Intensity Distribution of Time and Lethargy at x=1 and α=1

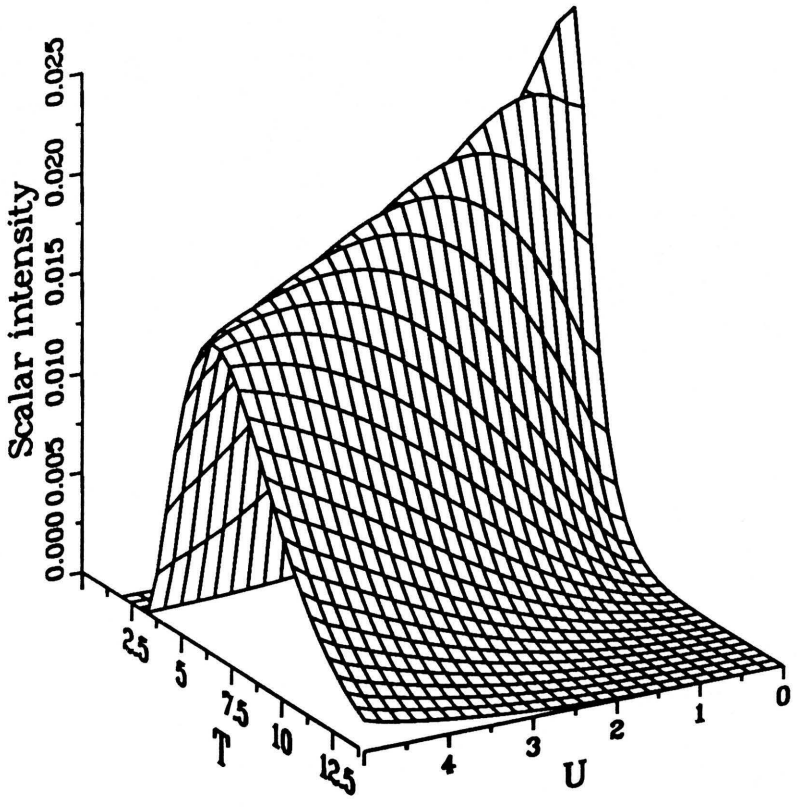

Figure 2.4b Intensity Distribution of Time and Lethargy at x=2 and α=1

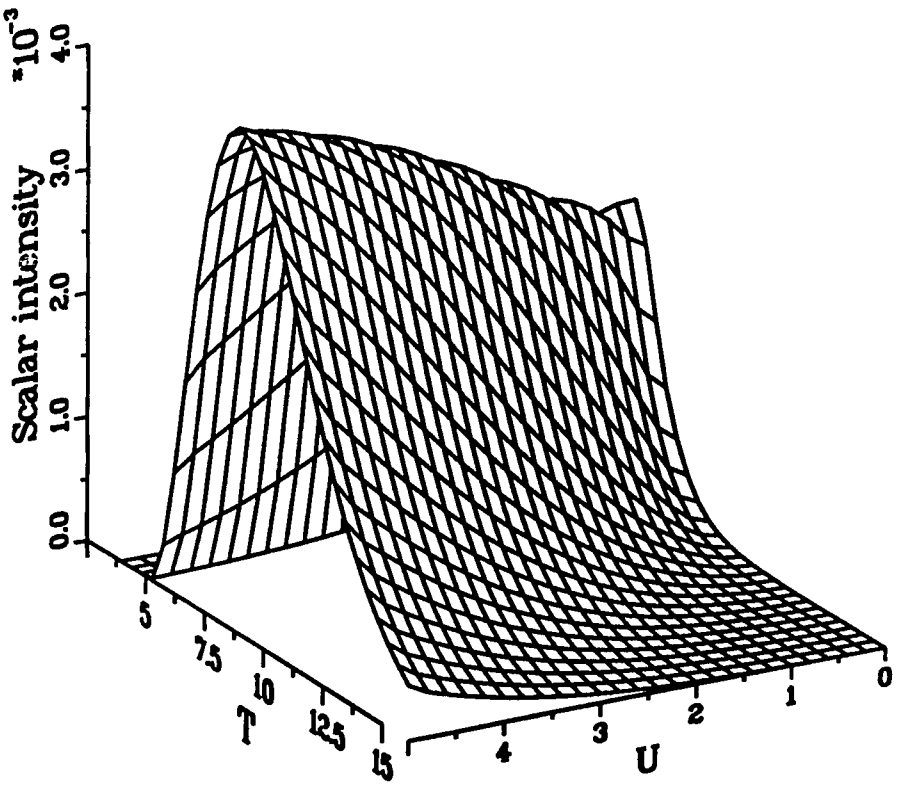

Figure 2.4c Intensity Distribution of Time and Lethargy at x=4 and α=1

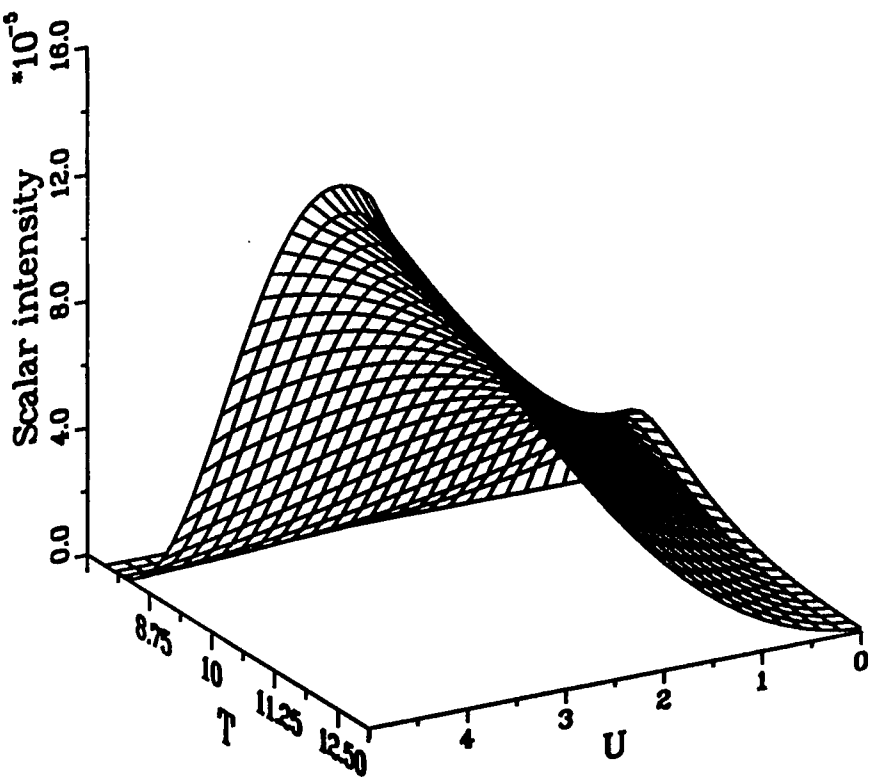

Figure 2.4d Intensity Distribution of Time and Lethargy at x=8 and α=1

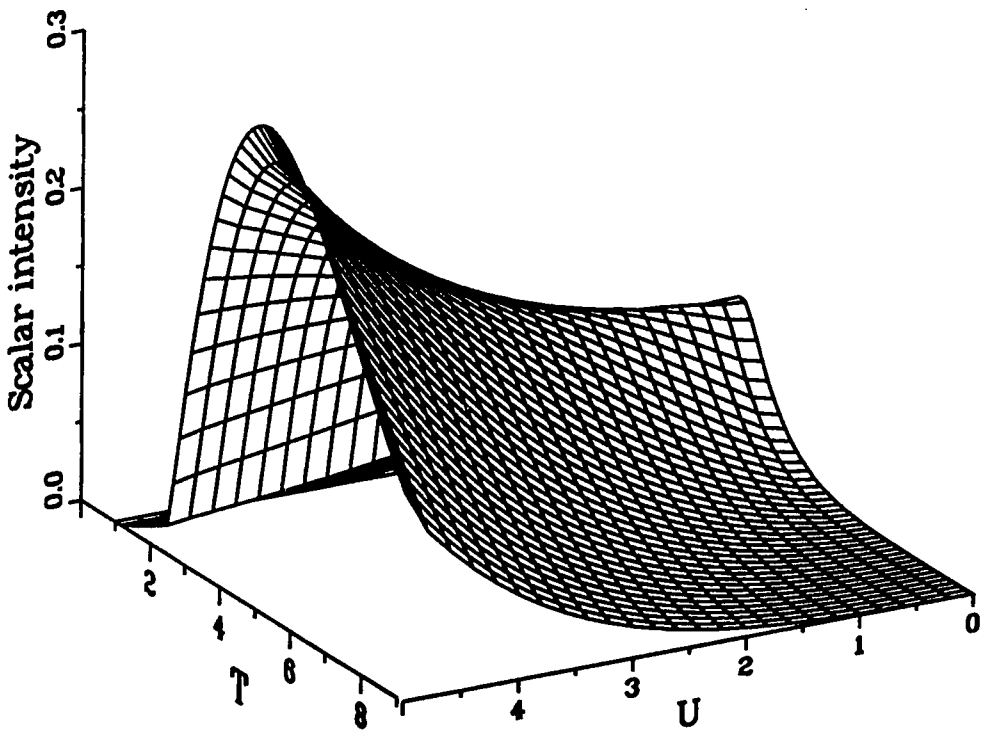

Figure 2.4e Intensity Distribution of Time and Lethargy at x=1 and α=0.5

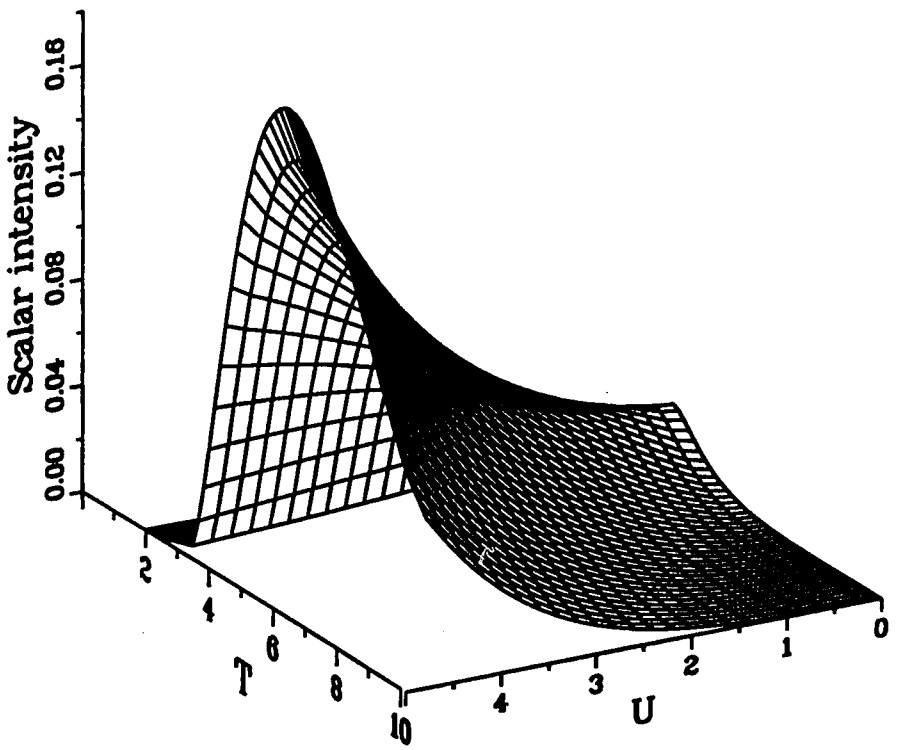

Figure 2.4f Intensity Distribution of Time and Lethargy at x=2 and α=0.5

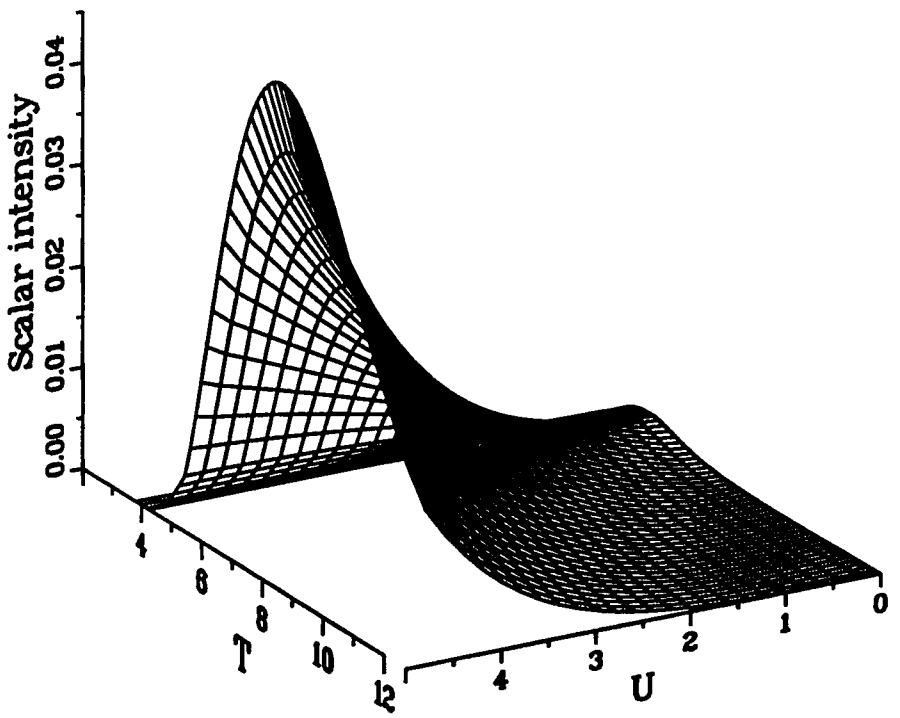

Figure 2.4g Intensity Distribution of Time and Lethargy at x=4 and α=0.5

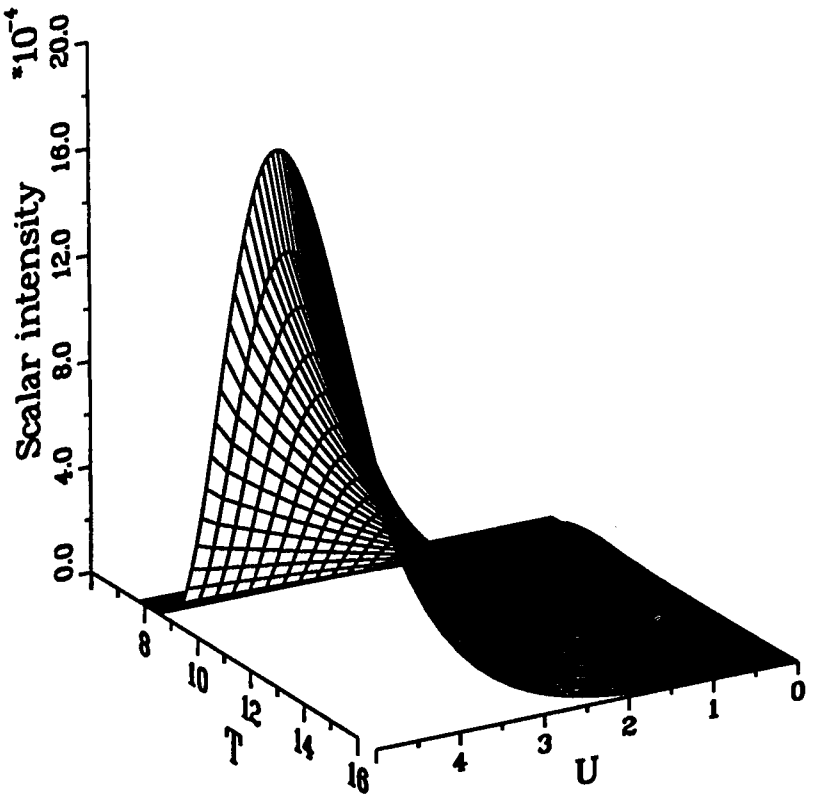

Figure 2.4h Intensity Distribution of Time and Lethargy at x=8 and α=0.5

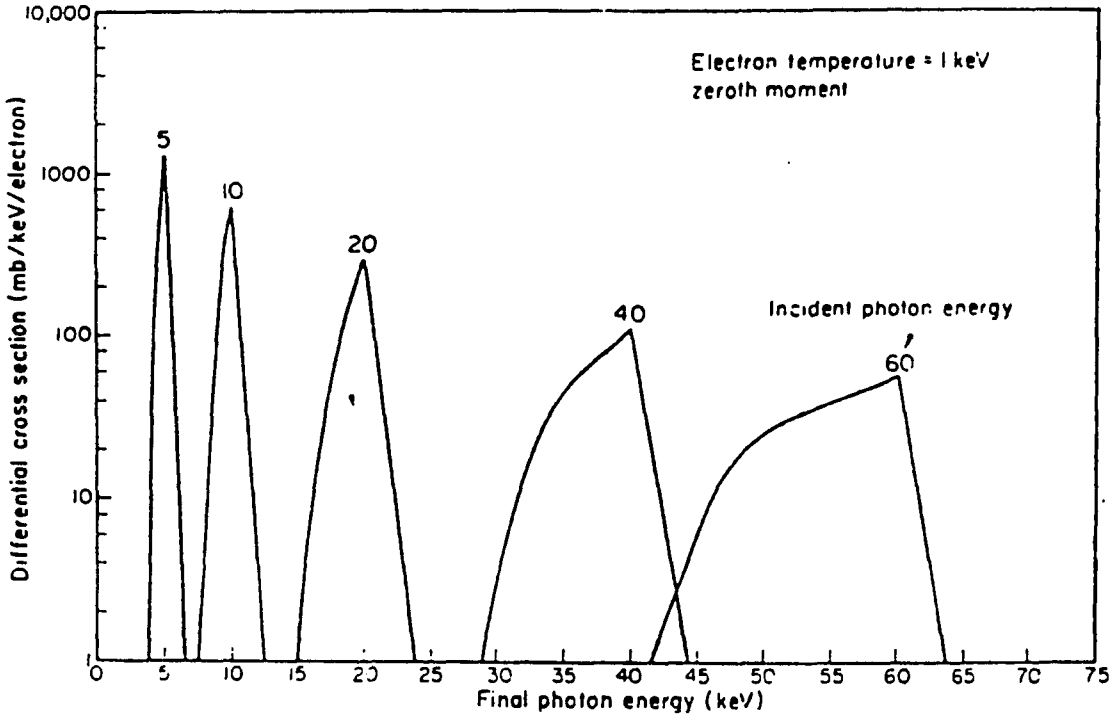

Figure 2.5a The Differential Scattering Cross-Section: n=0; T=1

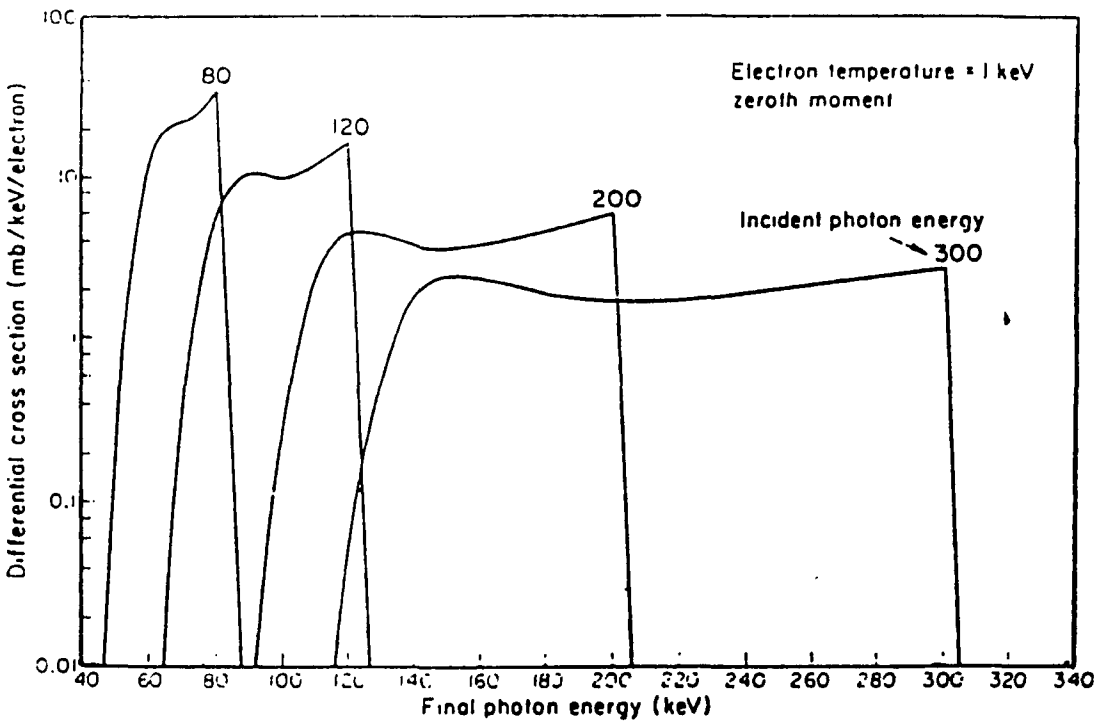

Figure 2.5b The Differential Scattering Cross-Section: n=0; T=1

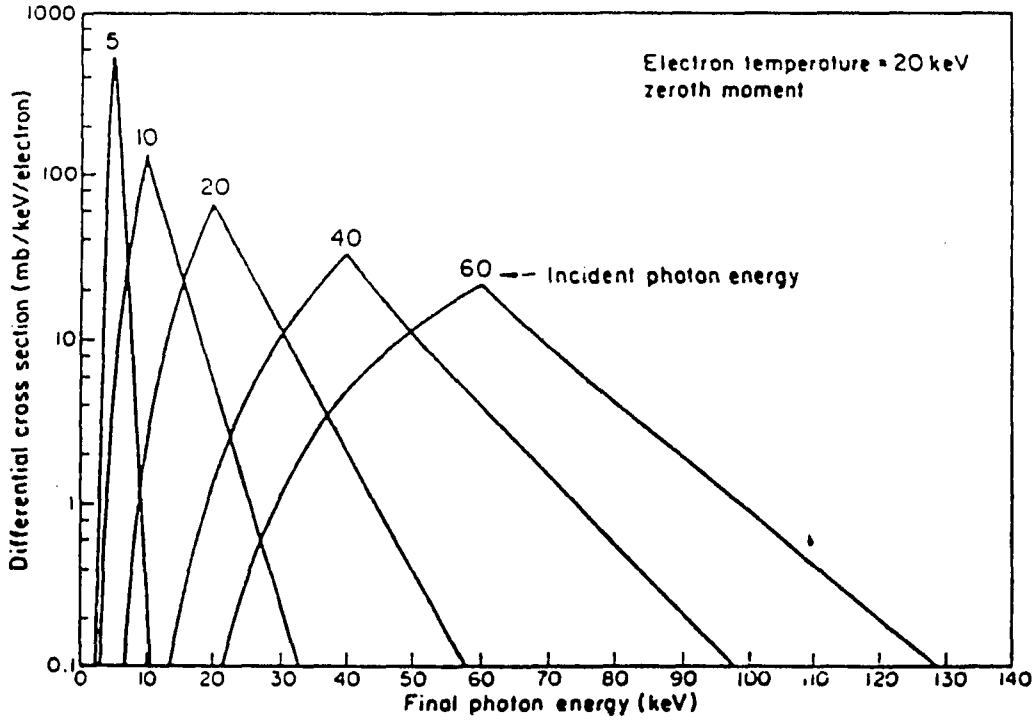

Figure 2.5c The Differential Scattering Cross-Section: n=0; T=20

CHAPTER 3.

TIME-DEPENDENT MULTIGROUP RADIATIVE TRANSFER

3.1 Derivation of Multigroup Equation

As stated in chapter 2, in an infinite isotropically scattering medium, the time dependent continuous lethargy radiative transfer equation is

$$\left[\frac{1}{c}\frac{\partial}{\partial t}+\mu\frac{\partial}{\partial x}+\sigma_t(u)\right]I(x,\mu,u,t)= \frac{1}{2}\int_{-1}^{1}d\mu'\int_{0}^{\infty}du'\sigma_s(u)f(u-u')I(x,\mu',u',t) + S(x,\mu,u,t) \tag{3.1}$$

$$\lim_{|x|\to\infty} I(x,\mu,u,t)=0$$

$$I(x,\mu,u,t)=0 \qquad t<0$$

where t and x are in physical units. The upper integral limit of lethargy on the right hand side was set to ∞ since $f(u)=0$ when $u<0$. $S(x,\mu,u,t)$ is the general photon source. To derive the multigroup equations, we first divide the lethargy range into G intervals. The photons in group g are taken to be just those with lethargy between u_{g-1} and u_g, hence the group number increases as the lethargy increases. Our

objective now is to obtain an approximation to the continuous lethargy transport equation in terms of the group intensity

$$I_g(x,\mu,t) = \int_{u_{g-1}}^{u_g} du I(x,\mu,u,t). \tag{3.2}$$

We proceed by dividing the lethargy integral in equation (3.1) into the contribution for each lethargy group and integrate equation (3.1) over the lethargy group $u \subset [u_{g-1}, u_g]$. The following equation results;

$$\frac{1}{c}\int_{u_{g-1}}^{u_g} du \frac{\partial}{\partial t} I(x,\mu,u,t) + \mu \int_{u_{g-1}}^{u_g} du \frac{\partial}{\partial x} I(x,\mu,u,t) + \int_{u_{g-1}}^{u_g} \sigma_t(u) I(x,\mu,u,t) = \frac{1}{2}\int_{-1}^{1} d\mu' \int_0^{\infty} du' \int_{u_{g-1}}^{u_g} du \sigma_s(u) f(u-u') I(x,\mu',u',t) + \int_{u_{g-1}}^{u_g} du S(x,\mu,u,t). \tag{3.3}$$

We now formally define the total group cross section and group source as:

$$\sigma_{tg} = \frac{1}{I_g(x,\mu,t)} \int_{u_{g-1}}^{u_g} du \sigma_t(u) I(x,\mu,u,t) \tag{3.4}$$

$$S_g(x,\mu,t) = \int_{u_{g-1}}^{u_g} du S(x,\mu,u,t). \tag{3.5}$$

Replacing the integral over u' on the right side of equation (3.3) by a sum of integrals of $u' \subset [u_{g'-1}, u_{g'}]$ over all the G groups gives;

$$\int_0^{\infty} du' \sigma_s(u) f(u-u') I(x,\mu',u',t) = \sum_{g'=1}^{G} \int_{u_{g'-1}}^{u_{g'}} du' \sigma_s(u) f(u-u') I(x,\mu',u',t). \tag{3.6}$$

Then if we assume that the source only occurs in the first group, Eq.(3.3) becomes;

$$\left[\frac{1}{c}\frac{\partial}{\partial t}+\mu\frac{\partial}{\partial x}+\sigma_{tg}\right]I_g(x,\mu,t)= \frac{1}{2}\int_{-1}^{1}d\mu'\int_{u_{g-1}}^{u_g}du\sum_{g'=1}^{G}\int_{u_{g'-1}}^{u_{g'}}du'\sigma_s(u)f(u-u')I(x,\mu',u',t) + S(x,\mu,t)\delta_{g1}, \tag{3.7}$$

where the group transfer cross section has been defined as;

$$\sigma_{sg'g}=\frac{1}{I_{g'}(x,\mu,t)}\int_{u_{g-1}}^{u_g}du\int_{u_{g'-1}}^{u_{g'}}du'\sigma_s(u)f(u-u')I(x,\mu',u',t). \tag{3.8}$$

So finally equation (3.3) becomes the standard multigroup equation;

$$\left[\frac{1}{c}\frac{\partial}{\partial t}+\mu\frac{\partial}{\partial x}+\sigma_{tg}\right]I_g(x,\mu,t)=\sum_{g'=1}^{G}\frac{1}{2}\sigma_{sg'g}\int_{-1}^{1}d\mu'I_{g'}(x,\mu',t) + S(x,\mu,t)\delta_{g1}. \tag{3.9}$$

For convenience, the time and position will be measured in terms of the mean-free-time and mean-free-path of the first group by letting $t\rightarrow t\sigma_{t1}c$ and $x\rightarrow x\sigma_{t1}$

$$\left[\frac{\partial}{\partial t}+\mu\frac{\partial}{\partial x}+\frac{\sigma_{tg}}{\sigma_{t1}}\right]I_g(x,\mu,t)=\sum_{g'=1}^{G}\frac{1}{2}\frac{\sigma_{sg'g}}{\sigma_{t1}}\int_{-1}^{1}d\mu'I_{g'}(x,\mu',t) + S_g(x,\mu,t)\delta_{g1}. \tag{3.10}$$

Note Eq. (3.10) is not applicable to space and time dependent cross section. If we let $\omega_g=\frac{\sigma_{tg}}{\sigma_{t1}}$ and $\omega_{sg'g}=\frac{\sigma_{sg'g}}{\sigma_{t1}}$, the multigroup radiative transfer equation is given by

$$\left[\frac{\partial}{\partial t}+\mu\frac{\partial}{\partial x}+\omega_g\right]I_g(x,\mu,t)=\sum_{g'=1}^{G}\frac{1}{2}\omega_{sg'g}\int_{-1}^{1}d\mu'I_{g'}(x,\mu',t) + S(x,\mu,t)\delta_{g1}. \tag{3.11}$$

Equation (3.11) is a general expression for both up-scattering and down-scattering cases. The group scalar intensity for only down-scattering case has been determined from the numerical evaluation of Eq. (3.11) with appropriate source in code TEMPSMG[14].

3.2 Brief Description of the Multigroup Solution

For completeness, the numerical evaluation of group scalar intensity in code TEMPSMG[14] will be described briefly in this section. For a source of the form $S(x,\mu,t) = \delta(x)\delta(\mu-\mu_0)\delta(t)$, The group intensity $I_g(x,\mu,t)$ in Eq. (3.11) can be expanded by the following multiple collision series

$$I_g(x,\mu,t) = \sum_{j=0}^{\infty} \lambda^j I_{j,g}(x,\mu,t). \tag{3.12}$$

When this expansion is introduced into Eq. (3.11), an infinite set of partial differential equations for the reduced group intensity $I_{j,g}(x,\mu,t)$ can be found. The general solution of $I_{j,g}$ can be obtained from integral transport theory

$$I_{j,g}(x,\mu,t) = \int_0^t dt' e^{-\omega_g(t-t')} q_{j,g}(x-\mu(t-t'),\mu,t') \tag{3.13a}$$

where

$$q_{0,g} = \delta(\mu-\mu_0)\delta(x)\delta(t)\delta_{g1}, \tag{3.13b}$$

$$q_{j,g} = \frac{1}{2}\sum_{g'=1}^{G} \omega_{g'g} \int_{-1}^{1} d\mu' I_{j-1,g'}(x,\mu',t), \qquad j \geq 1. \tag{3.13c}$$

The uncollided contribution (n=0) then becomes

$$I_{0,g}(x,\mu,t) = \frac{e^{-t}}{t}\delta(\mu-\mu_0)\delta(\mu-\eta)\delta_{g1}. \tag{3.14}$$

By means of induction, the group intensity can be shown to be

$$I_g(x,\mu,t) = I_{0g}(x,\mu,t) + \sum_{n=1}^{\infty} \frac{t^{n-1}}{n!} \xi_n^g(\mu,\eta). \tag{3.15}$$

The first term on right hand side of Eq. (3.15) is the uncollided contribution and second term is the collided contribution. Since the wave front initiated by the source in the first group is inherited by all succeeding groups ($|\eta| \leq 1$), the scalar component $\xi_n^g(\eta)$ can be expanded by Legendre polynomial in oder to evaluate the group scalar intensity $I_g(x,t)$.

$$\xi_n^g(\eta) = \sum_{k=0}^{\infty} \frac{2k+1}{2} \xi_{n,k}^{0,g} P_k(\eta) \tag{3.16}$$

where

$$\xi_{n,k}^{l,g} = \int_{-1}^{1} d\mu P_l(\mu) \int_{-1}^{1} d\eta P_k(\eta) \xi_n^g(\mu,\eta). \tag{3.17}$$

A coupled set of algebraic equations for the moments $\xi_{n,k}^{l,g}$ has been obtained to determine the expansion coefficients $\xi_{n,k}^{0,g}$.

$$\begin{aligned}(k+n)\xi_{n,k}^{l,g} &= -(k-n-1)\xi_{n,k-2}^{l,g} + \frac{2k-1}{2k+1}[(l+1)\xi_{n,k-1}^{l+1,g} + l\xi_{n,k-1}^{l-1,g}] \\ &+ n[\omega_{sg'g}\delta_{l,0} - \omega_g][\xi_{n-1,k}^{l,g} - \xi_{n-1,k-2}^{l,g}] + n\sum_{g'=1}^{G} \omega_{sg'g}[\xi_{n-1,k}^{0,g'} - \xi_{n-1,k-2}^{0,g'}]\end{aligned} \tag{3.18}$$

The starting value for this four-level recursion relation is the moment n=0

$$\xi_{0,k}^{l,g} = \delta_{g1} \frac{\delta_{k,l}}{2k+1} \tag{3.19}$$

and the moment for k=0

$$\xi_{n,0}^{l,g} = (-1)^n \psi_{n,g}^l \tag{3.20a}$$

where

$$\psi_{0,g}^l = Q_l \delta_{g1}, \qquad Q_l = \int_{-1}^{1} d\mu P_l(\mu)\delta(\mu - \mu_0) \tag{3.20b}$$

$$\psi^l_{n,g} = \omega_g \psi^l_{n-1,g} - \delta_{l0} \sum_{g'=1}^{G} \omega_{sg'g} \psi^l_{n-1,g'}. \qquad (3.20c)$$

The procedure of numerical evaluation of group scalar intensity in Eq. (3.15) is same to one-group case except the expansion coefficient satisfies a four-level recursion relation.

3.3 Determination of Group Parameters

Before the multigroup transport calculations can be carried out, values of the multigroup cross sections σ_{tg} and $\sigma_{sg'g}$ must be made avaliable. As indicated by the definition in equation (3.4) and (3.8), however, the evaluation of group cross sections requires that both the detailed lethargy dependence of the cross section and the spectral intensity (or weighting function) be known. For simplicity we assume that the cross section is independent of lethargy. This is done in order to compare to the analytical solution. Assume the lethargy dependence of the angular photon intensity for each lethargy group is seperable and can be approximated as the product of a known function of lethargy $w(u)$ and the group intensity $I_g(x, \mu, t)$

$$I(x, \mu, u, t) = I_g(x, \mu, t) w(u), \qquad u_{g-1} < u < u_g. \qquad (3.21)$$

The energy dependent spectral weighting function $w(u)$ is normalized by definition of group intensity to

$$\int_g w(u) du = 1, \qquad (3.22a)$$

where $\int_g$ is defined as the integral over lethargy of group g ($u_{g-1} \leq u \leq u_g$). The simplest case is to assume that

$$w(u) = \frac{1}{\Delta u_g} \qquad u_{g-1} \leq u \leq u_g \qquad (3.22b)$$

so we have for the group cross section and group transfer cross section

$$\omega_g = \frac{\sigma_{tg}}{\sigma_{t1}} = 1 \tag{3.23}$$

and

$$\omega_{sg'g} = \frac{\sigma_{sg}}{\sigma_{t1}} \frac{1}{\Delta u_g} \int_g du \int_{g'} du' f(u-u'). \tag{3.24}$$

Recall that for the special scattering kernel used in continuous lethargy calculation, $f(u-u') = e^{-\alpha(u-u')}\theta(u-u')$.

When $g = g'$ then the within group transfer cross section is

$$\begin{aligned} \omega_{sg'g} &= \frac{\sigma_s g}{\sigma_t 1} \frac{1}{\Delta u_g} \int_g du \int_{g'} du' e^{-\alpha(u-u')}\theta(u-u') \\ &= \frac{\sigma_{sg}}{\sigma_{t1}} \frac{1}{\alpha}[1 + \frac{1}{\alpha \Delta u_g}[e^{-\alpha(u_g - u_{g-1})} - 1]]. \end{aligned} \tag{3.25}$$

When $g > g'$

$$\begin{aligned} \omega_{sg'g} &= \frac{\sigma_{sg}}{\sigma_{t1}} \frac{1}{\Delta u_{g'}} \int_g du \int_{g'} du' e^{-\alpha(u-u')}\theta(u-u') \\ &= \frac{\sigma_{sg}}{\sigma_{t1}} \frac{1}{\alpha^2 \Delta u_{g'}} (e^{-\alpha u_{g-1}} - e^{-\alpha u_g})(e^{\alpha u_{g'}} - e^{\alpha u_{g'-1}}). \end{aligned} \tag{3.26}$$

These multigroup cross section will be used in Eq (3.11) for comparison with the benchmark solution in the following chapter.

3.4 Generation of One-Group Results from Multigroup Equation

In order to demonstrate the accuracy of multigroup approximation method, we can sum all the group scalar intensities together to yield

$$I(x,t) = \sum_{g=1}^{G} I_g(x,t). \tag{3.27}$$

From Eq. (3.11), this result should be identical to the one-group solution when

$$\omega_g = 1, \qquad \sum_{g=1}^{G} \omega_{sg'g} = 1. \tag{3.28}$$

In the following procedure the derivation of one-group equation satisfied by I(x,t) (from continuous lethargy transport equation) is presented. If the one-group angular scalar intensity is defined as

$$I(x,\mu,t) = \int_0^\infty du I(x,\mu,u,t), \tag{3.29}$$

the following equation can be obtained from Eq. (3.1) with constant cross sections by integrating over lethargy u

$$\left[\frac{1}{c}\frac{\partial}{\partial t} + \mu\frac{\partial}{\partial x} + \sigma_t\right] I(x,\mu,t) = \frac{1}{2}\int_{-1}^{1} d\mu' \int_0^\infty du' \int_0^\infty du \sigma_s f(u-u') I(x,\mu',u',t) + \int_0^\infty du S(x,\mu,u,t). \tag{3.30}$$

For the scattering kernel $f(u-u') = e^{-\alpha(u-u')}$ normalized to $\frac{1}{\alpha}$, we obtain the one-group time dependent equation;

$$\left[\frac{\partial}{\partial t} + \mu\frac{\partial}{\partial x} + 1\right] I(x,\mu,t) = \frac{\omega}{2\alpha}\int_{-1}^{1} d\mu' I(x,\mu',t) + S(x,\mu,t), \tag{3.31}$$

where $x \to \sigma_t x$ and $t \to \sigma_t ct$. The equation (3.31) can be solved by the direct application of code TEMPS[11] with appropripate source in order to check the accuracy of multigroup calculation which will be done in next chapter.

CHAPTER 4.

NUMERICAL RESULTS AND DISSCUSSION

To check the accuarcy of multigroup calculations, the scattering kernel $f(u-u') = e^{-\alpha(u-u')}\theta(u-u')$ has been used. A fictitious multigroup problem equivalent to the one-group problem has been tested by setting

$$\omega_g = 1, \qquad \sum_{g'=1}^{G} \omega_{sg'g} = 1, \tag{4.1}$$

and by summing all the group scalar intensity

$$I(x,t) = \sum_{g=1}^{G} I_g(x,t). \tag{4.2}$$

The result must be equivalent to the one-group solution I(x,t) of equation (3.31) for all cross sections set to unity with the number of secondaries replaced by ω/α. For a purely down scattering problem with five groups (G=5) and a seires truncation error 10^{-4} and $\alpha = 1.0$, the comparison of equation (4.2) with the solution of equation (3.31) shows a difference in the fourth place. Table (4.1) gives one example of the

comparison of the five-group and one-group results at t=1.

Table 4.1
Comparison of the Multigroup
with One-Group Results
at t=1

X	Multigroup	One-Group
0.01	6.7542E − 01	6.7541E − 01
0.11	6.6814E − 01	6.6811E − 01
0.21	6.4899E − 01	6.4892E − 01
0.31	6.1845E − 01	6.1841E − 01
0.41	5.7757E − 01	5.7754E − 01
0.51	5.2754E − 01	5.2753E − 01
0.61	4.6982E − 01	4.6980E − 01
0.71	4.0584E − 01	4.0584E − 01
0.81	3.3693E − 01	3.3690E − 01
0.91	2.6319E − 01	2.6321E − 01
1.01	0.0000E + 00	0.0000E + 00

As a demenstration, a few group calculation (G=3) is presented in figures 4.1a-d. It is found that as time increases the group intensity profile becomes depopulated in lower lethargy group and increases in higher lethargy group.

Figures 4.2a-g present the comparison of ten group (G=10, the first and last groups excluded) scalar intensity with the analytical solution for the continuous lethargy. Figures 4.2h-n for G=23. Excellent agreement is observed for multigroup calculation and continuous lethargy benchmark. In addition, as the number of multigroups increases, better agreement is observed.

Figures 4.3a and 4.3b show the comparison of multigroup results of a particular group u [0.1,1] with the results of integrating the continuous scalar intensity over that lethargy group interval. The trapezoidal rule,

$$I_g(x,t) = \int_a^b I(x,u,t)du$$
$$= \Delta u[\frac{I(x,a,t)+I(x,b,t)}{2} + \sum_{i=1}^{N-1} I(x,u_i,t)], \qquad (4.3)$$

is applied to perform the integration. The results also show excellent agreement between the multigroup scalar intensity and analytical continuous lethargy scalar intensity.

In addition, the group structure for ten-group calculation is presented in table (4.2) and group transfer cross section for ten-group is shown in table (4.3).

Table 4.2
Group Structure for G=10

g	u_{g-1}	u_g	Δu_g
1	0.0	0.1	0.1
2	0.1	0.7	0.6
3	0.7	1.3	0.6
4	1.3	1.9	0.6
5	1.9	2.5	0.6
6	2.5	3.0	0.5
7	3.0	3.5	0.5
8	3.5	4.0	0.5
9	4.0	4.5	0.5
10	4.5	50000.0	49995.5

Table 4.3a
Group Transfer Cross-Section for G=10

	$\omega_{sg'g}$			
g'	g=1	g=2	g=3	g=4
1	4.837E − 02	4.294E − 01	2.356E − 01	1.293E − 01
2	0.000E + 00	2.480E − 01	3.393E − 01	1.862E − 01
3	0.000E + 00	0.000E + 00	2.480E − 01	3.393E − 01
4	0.000E + 00	0.000E + 00	0.000E + 00	3.393E − 01
5	0.000E + 00	0.000E + 00	0.000E + 00	0.000E + 00
6	0.000E + 00	0.000E + 00	0.000E + 00	0.000E + 00
7	0.000E + 00	0.000E + 00	0.000E + 00	0.000E + 00
8	0.000E + 00	0.000E + 00	0.000E + 00	0.000E + 00
9	0.000E + 00	0.000E + 00	0.000E + 00	0.000E + 00
10	0.000E + 00	0.000E + 00	0.000E + 00	0.000E + 00

Table 4.3b
Group Transfer Cross-Section for G=10
(Continued)

	$\omega_{sg'g}$			
g'	g=5	g=6	g=7	g=8
1	7.097E − 02	3.397E − 02	2.060E − 02	1.250E − 02
2	1.022E − 01	4.891E − 02	2.966E − 02	1.799E − 02
3	1.862E − 01	8.912E − 02	5.405E − 02	3.278E − 02
4	3.393E − 01	1.624E − 01	9.849E − 02	5.974E − 02
5	2.480E − 01	2.959E − 01	1.795E − 01	1.088E − 01
6	0.000E + 00	2.131E − 01	3.096E − 01	1.878E − 01
7	0.000E + 00	0.000E + 00	2.131E − 01	3.096E − 01
8	0.000E + 00	0.000E + 00	0.000E + 00	2.131E − 01
9	0.000E + 00	0.000E + 00	0.000E + 00	0.000E + 00
10	0.000E + 00	0.000E + 00	0.000E + 00	0.000E + 00

Table 4.3c

Group Transfer Cross-Section for G=10

(Continued)

	$\omega_{sg'g}$	
g'	$g = 9$	$g = 10$
1	7.579E − 03	1.168E − 02
2	1.091E − 02	1.682E − 02
3	1.988E − 02	3.065E − 02
4	3.623E − 02	5.585E − 02
5	6.602E − 02	1.018E − 01
6	1.139E − 01	1.756E − 01
7	1.878E − 01	2.895E − 01
8	3.096E − 01	4.773E − 01
9	2.131E − 01	7.869E − 01
10	0.000E + 00	1.000E + 00
10	0.000E + 00	1.000E + 00

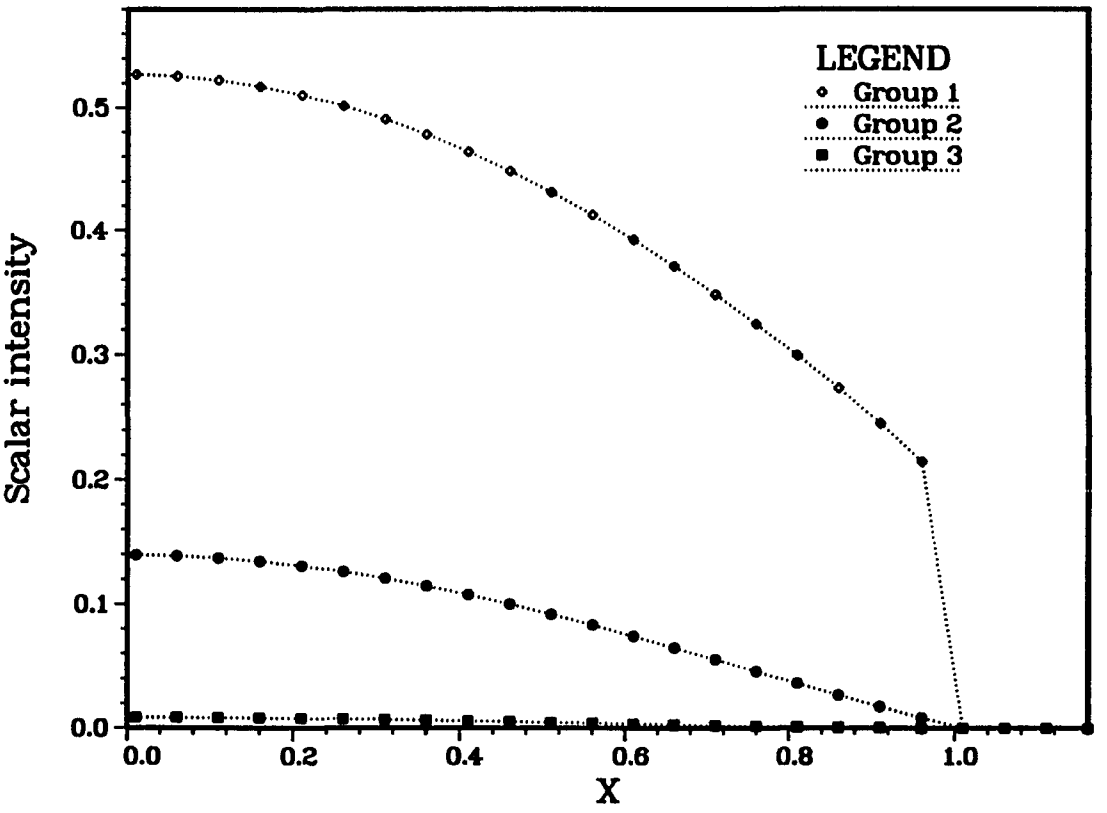

Figure 4.1a Multigroup Scalar Intensity Profile at t=1 with $\alpha = 1.0$

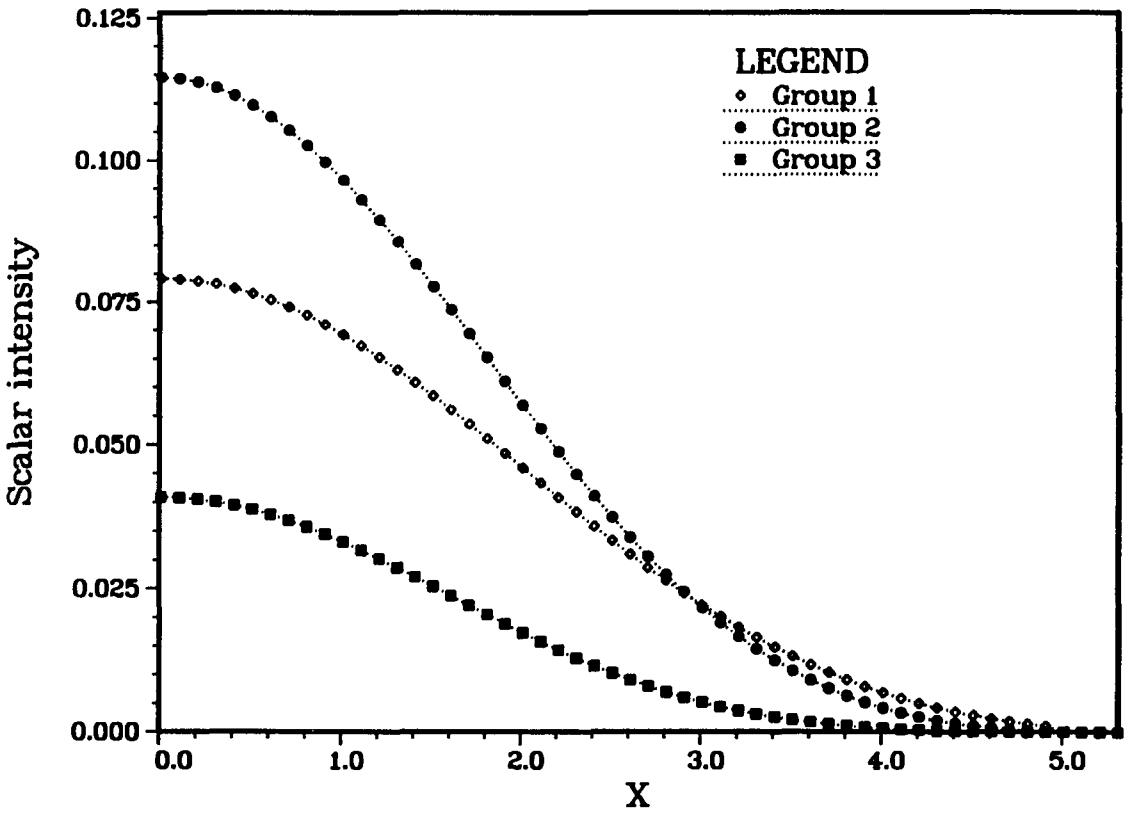

Figure 4.1b Multigroup Scalar Intensity Profile at t=5 with $\alpha = 1.0$

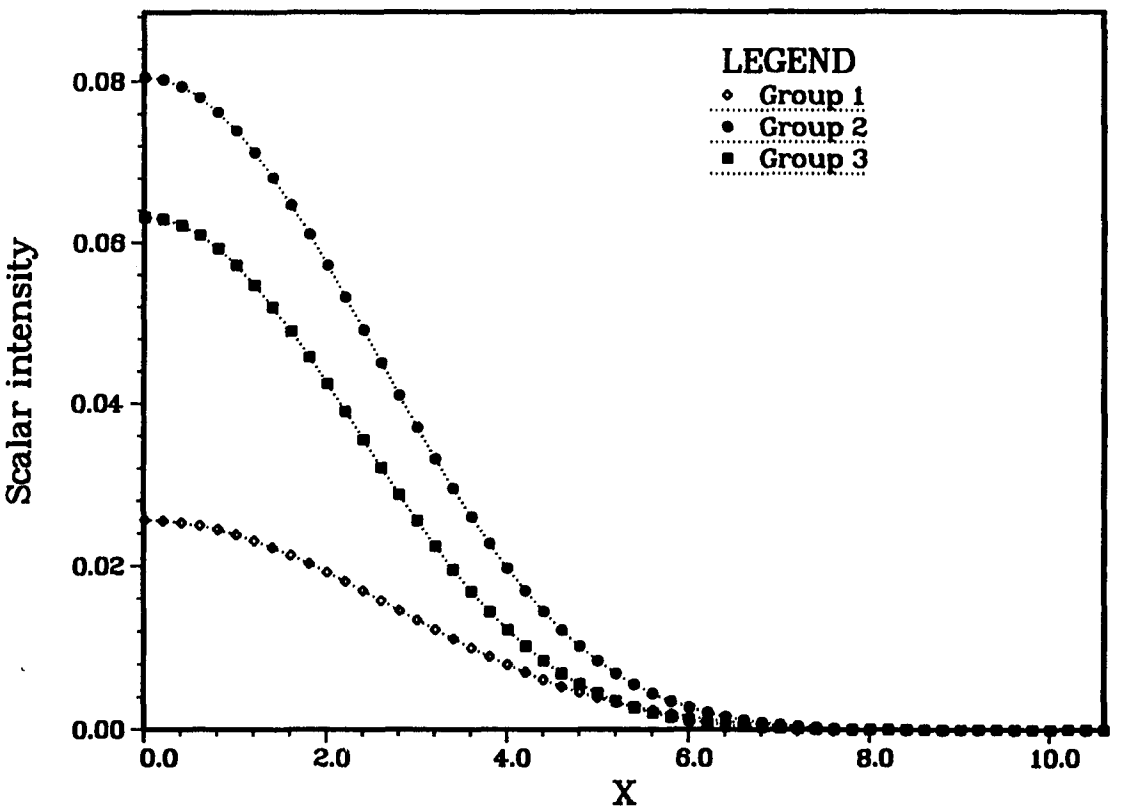

Figure 4.1c Multigroup Scalar Intensity Profile at t=9 with $\alpha = 1.0$

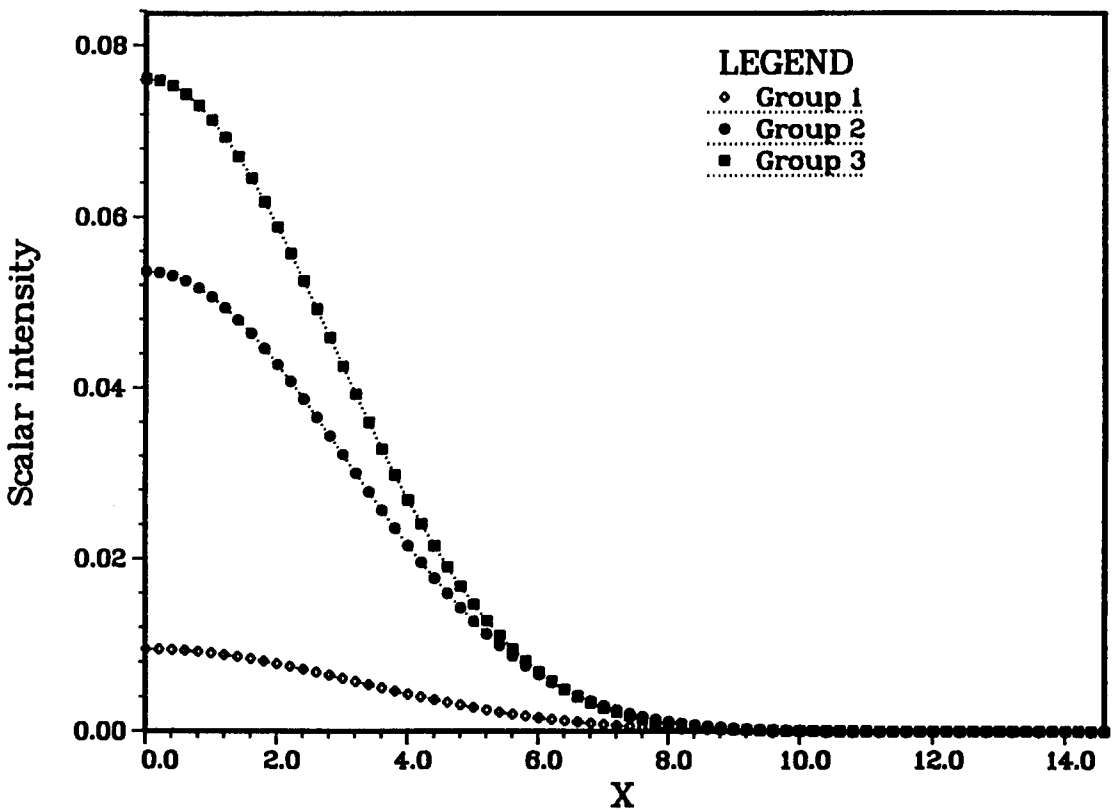

Figure 4.1d Multigroup Scalar Intensity Profile at t=13 with $\alpha = 1.0$

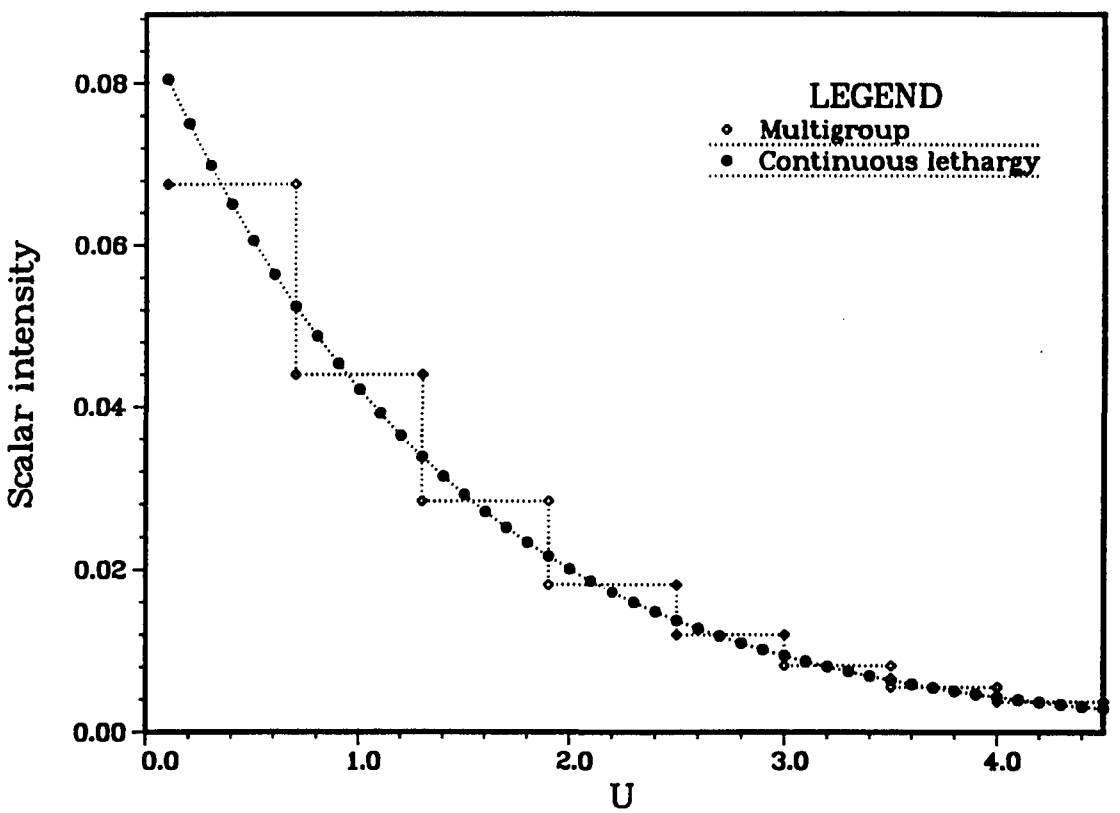

Figure 4.2a Comparison of Ten Group and Continuous Lethargy Results, t=1.2 at x=1

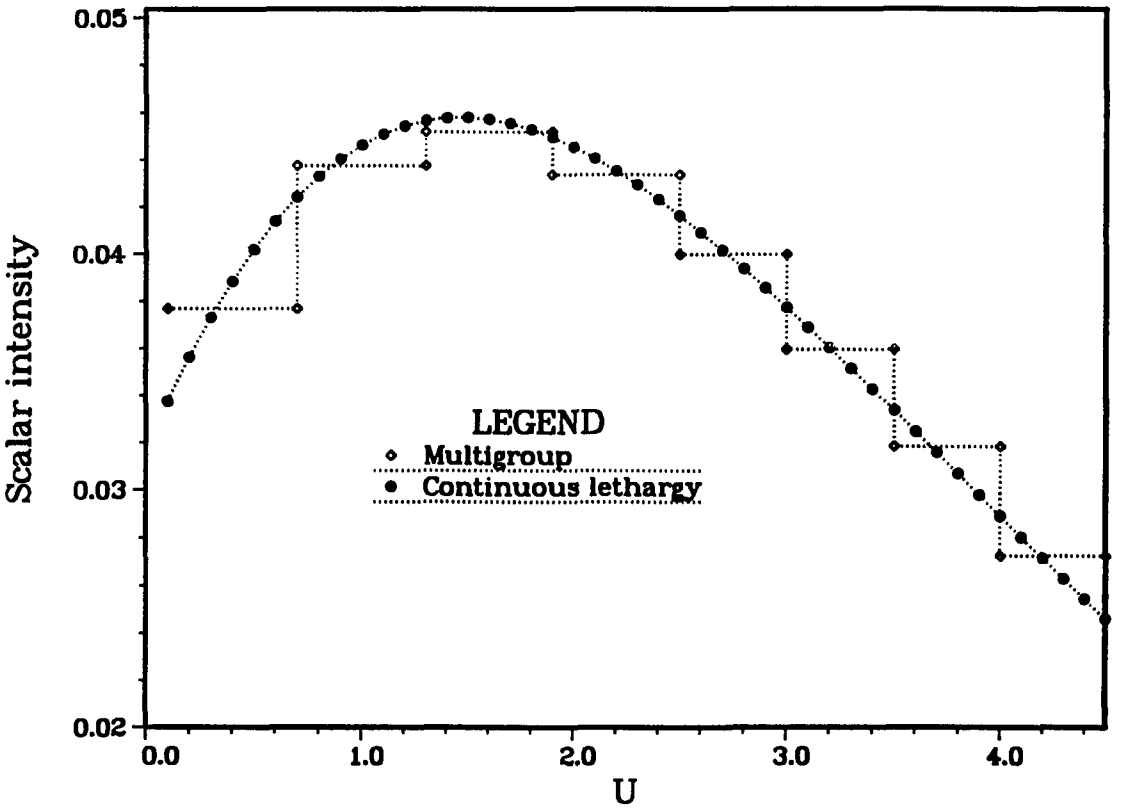

Figure 4.2b Comparison of Ten Group and Continuous Lethargy Results, t=3 at x=1

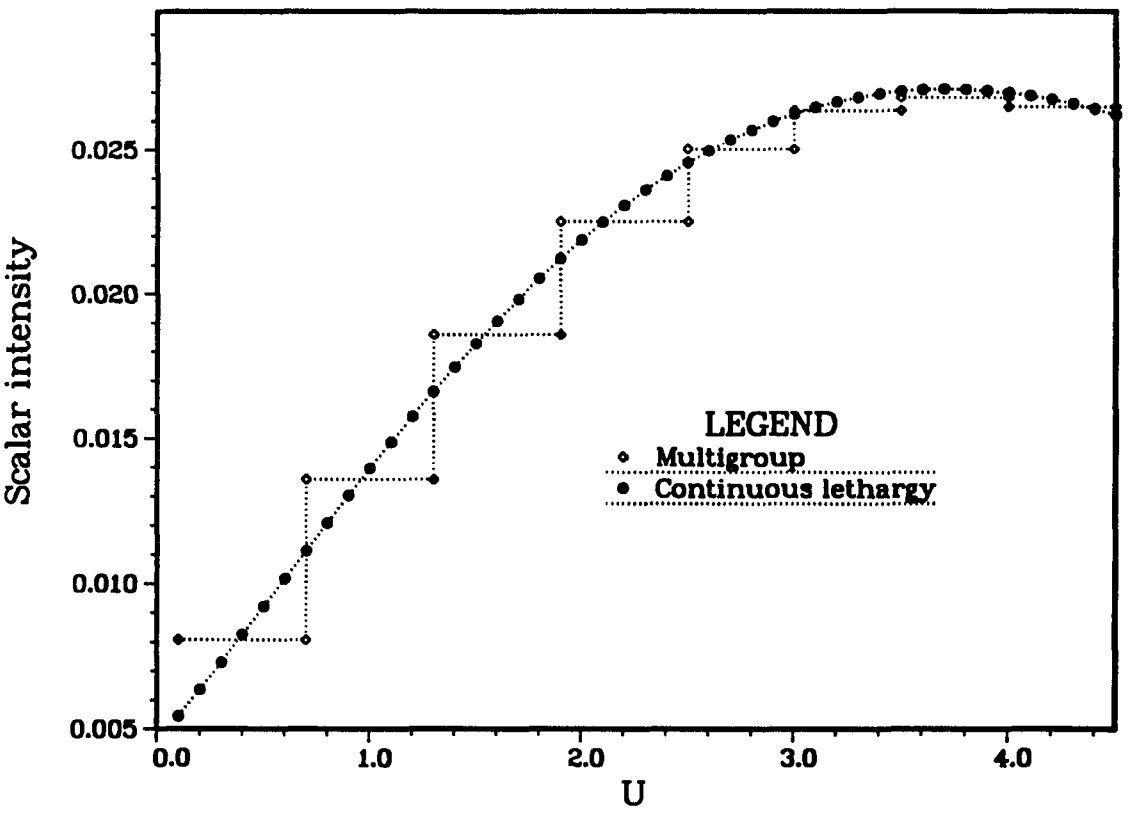

Figure 4.2c Comparison of Ten Group and Continuous Lethargy Results, t=5 at x=1

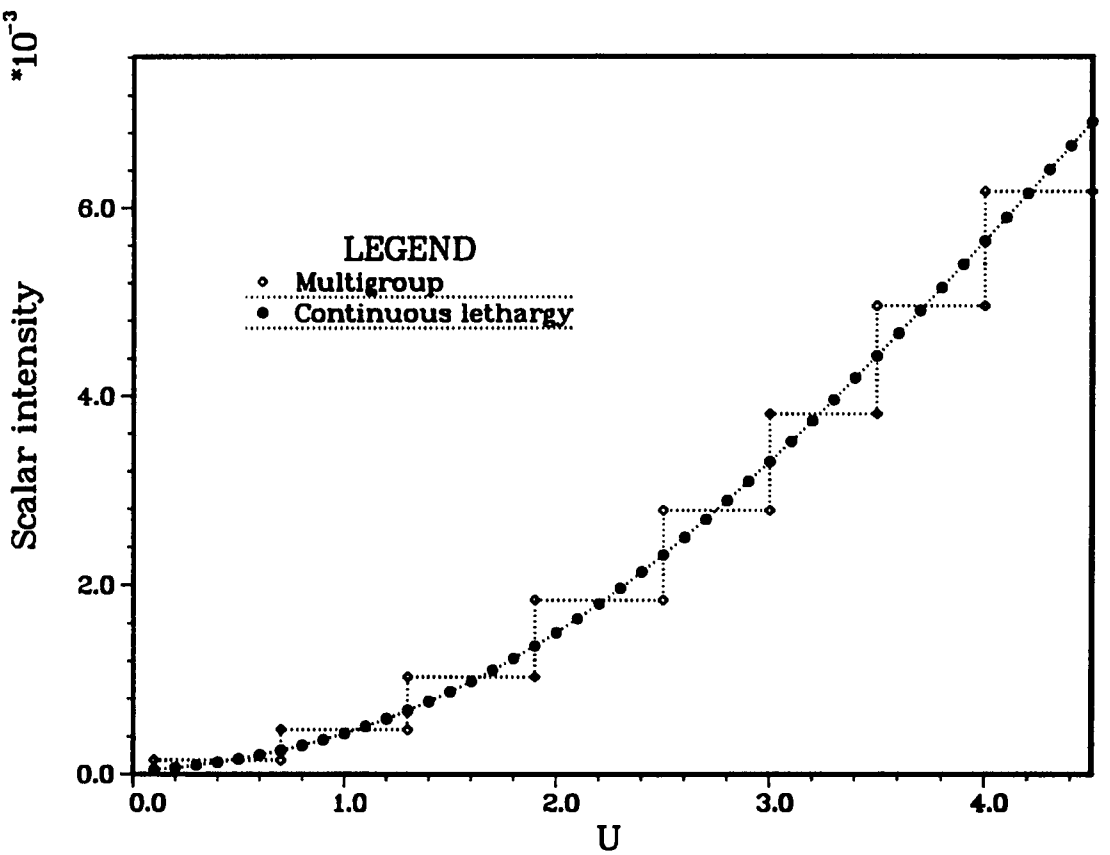

Figure 4.2d Comparison of Ten Group and Continuous Lethargy Results, t=10 at x=1

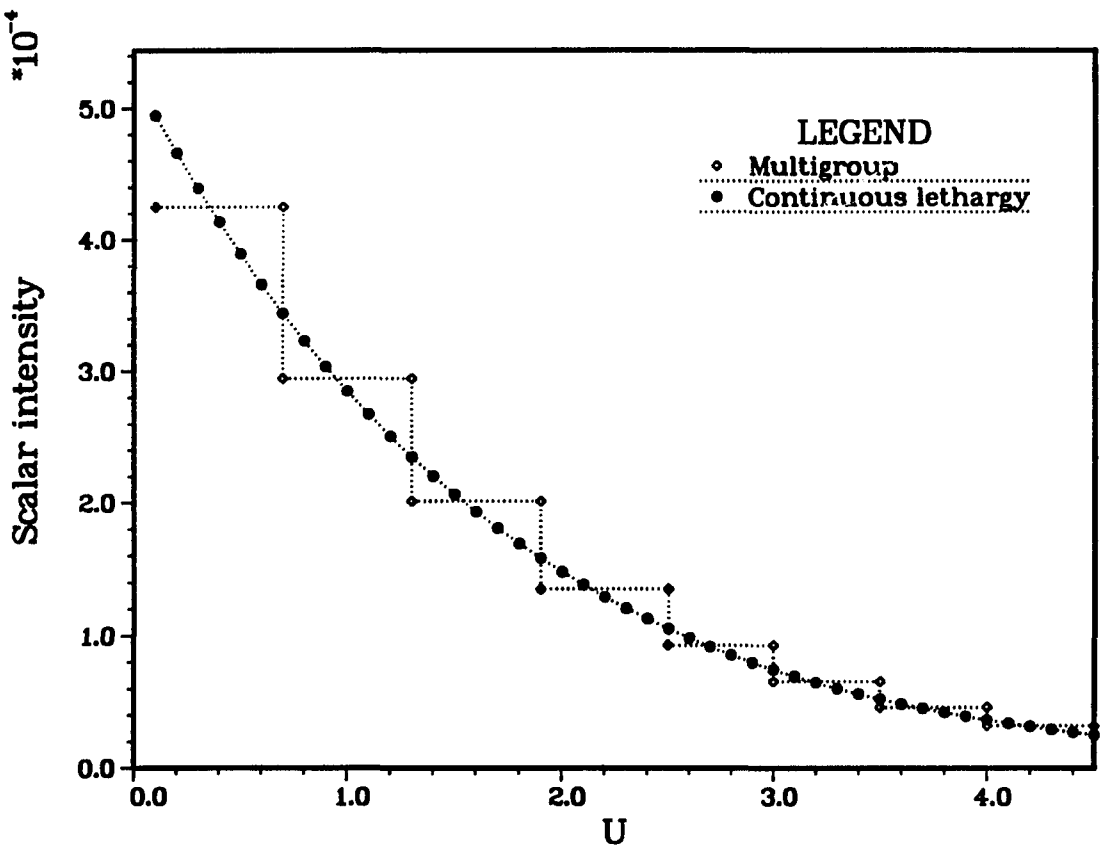

Figure 4.2e Comparison of Ten Group and Continuous Lethargy Results, t=5.2 at x=5

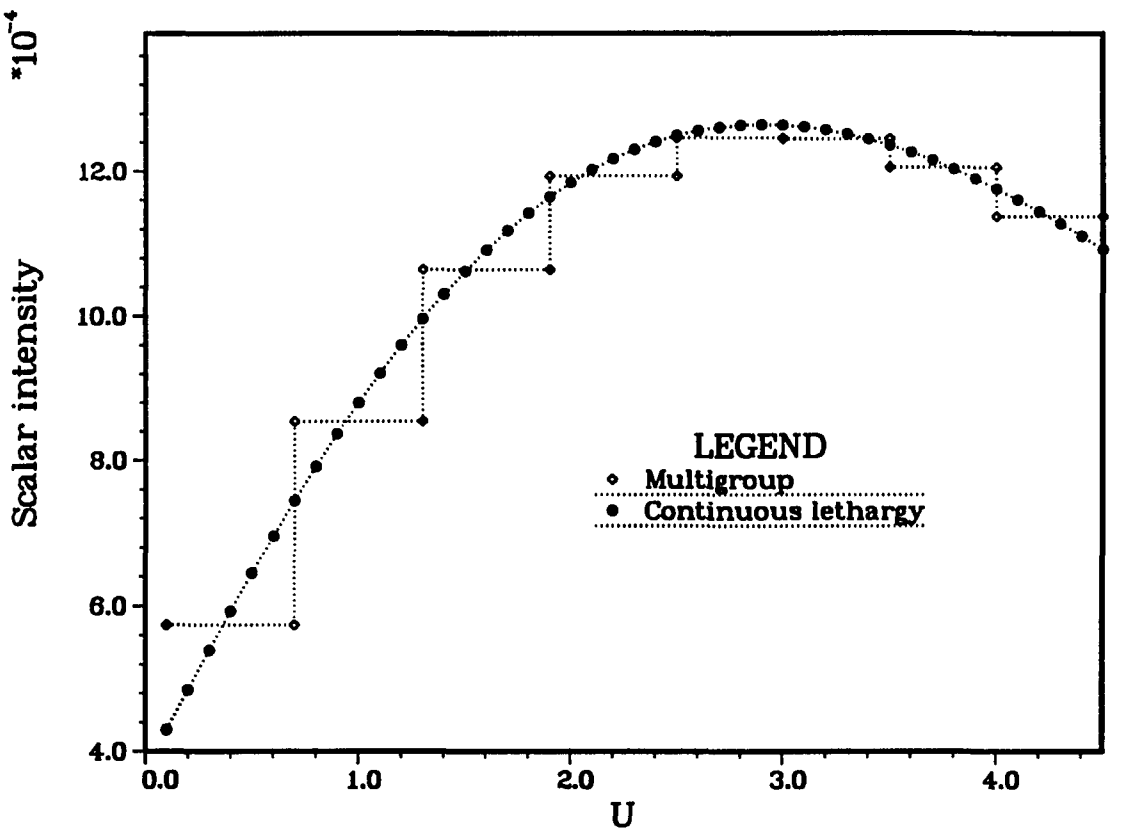

Figure 4.2f Comparison of Ten Group and Continuous Lethargy Results, t=7 at x=5

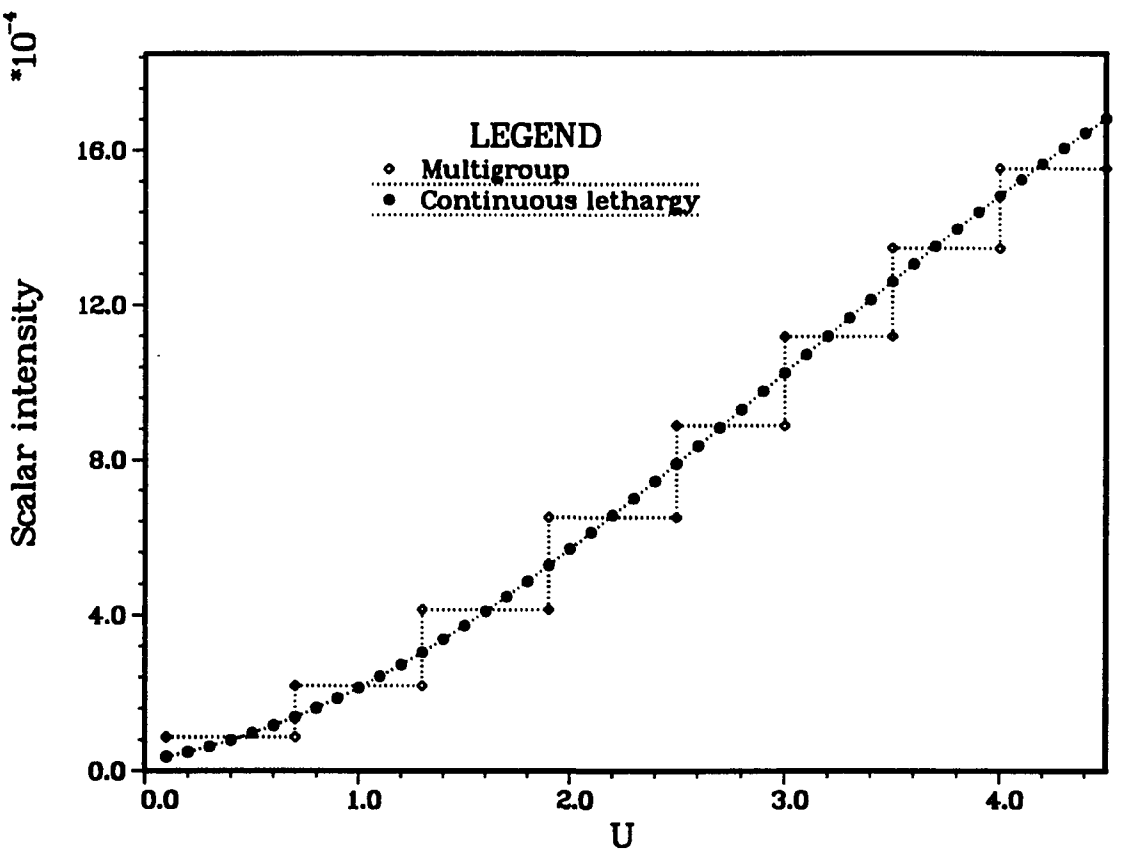

Figure 4.2g Comparison of Ten Group and Continuous Lethargy Results, t=10 at x=5

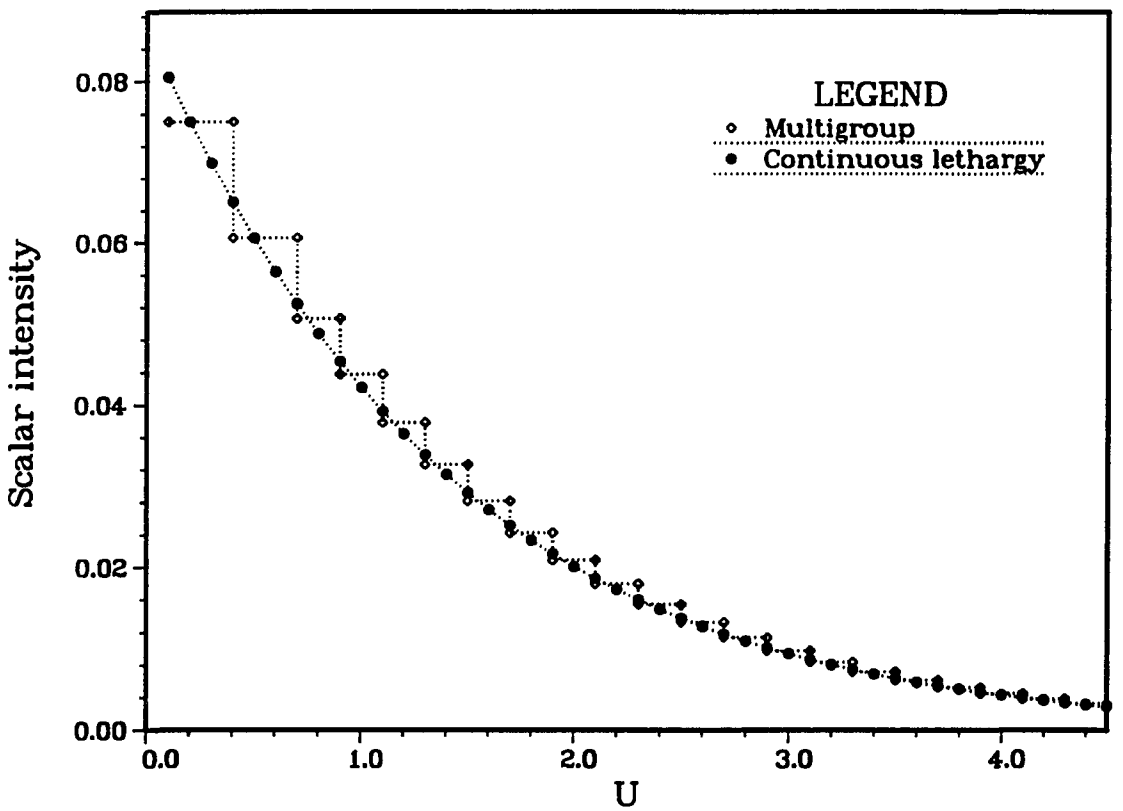

Figure 4.2h Comparison of Twenty-Three Group and Continuous Lethargy Results, t=1.2 at x=1

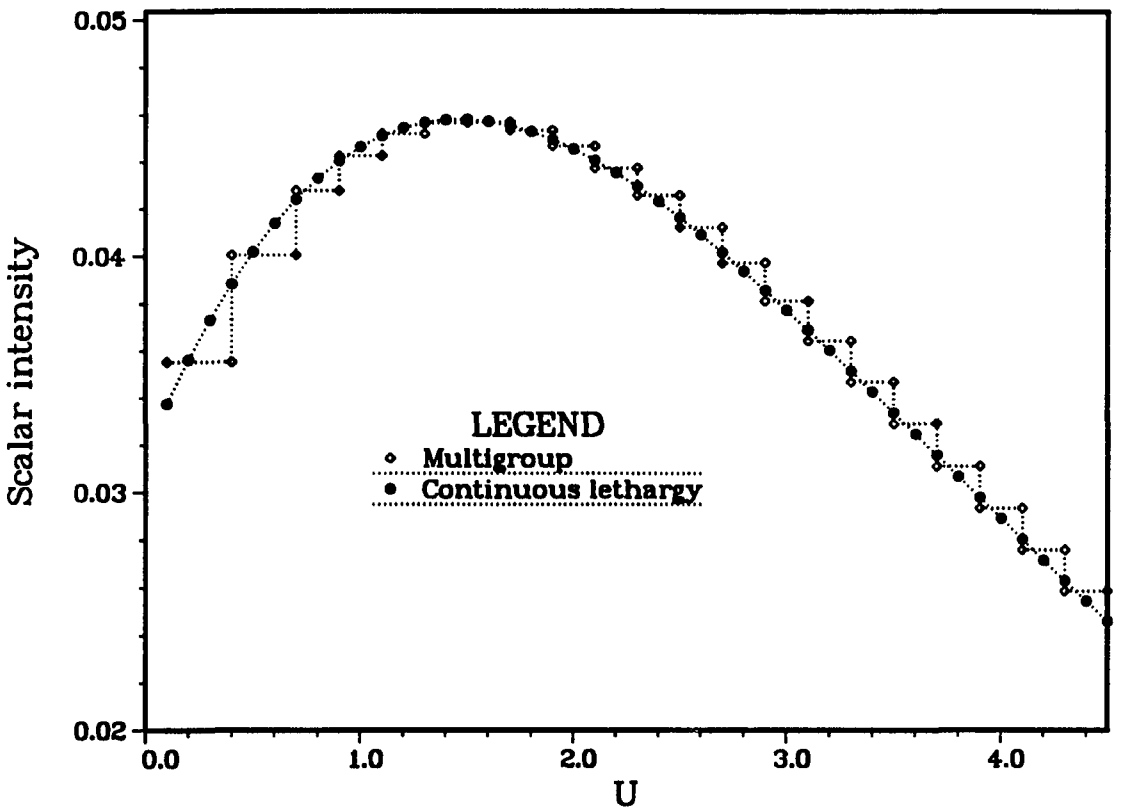

Figure 4.2i Comparison of Twenty-Three Group and Continuous Lethargy Results, t=3 at x=1

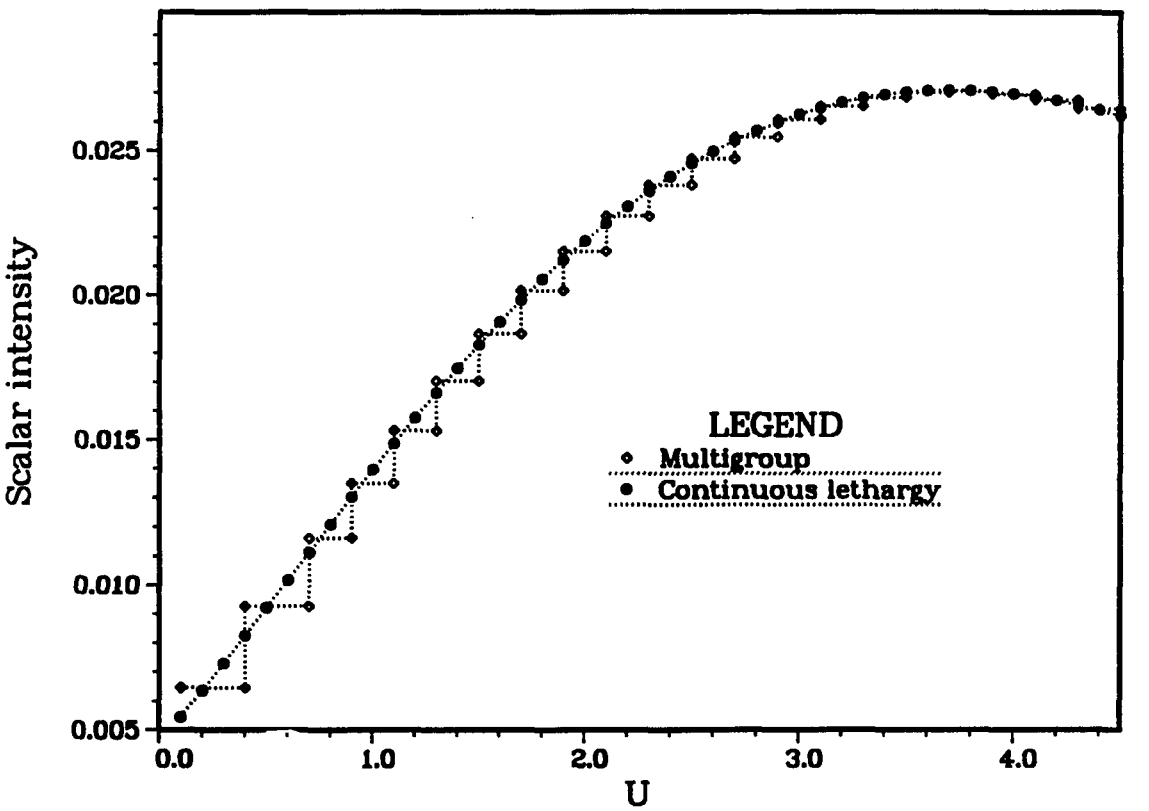

Figure 4.2j Comparison of Twenty-Three Group and Continuous Lethargy Results, t=5 at x=1

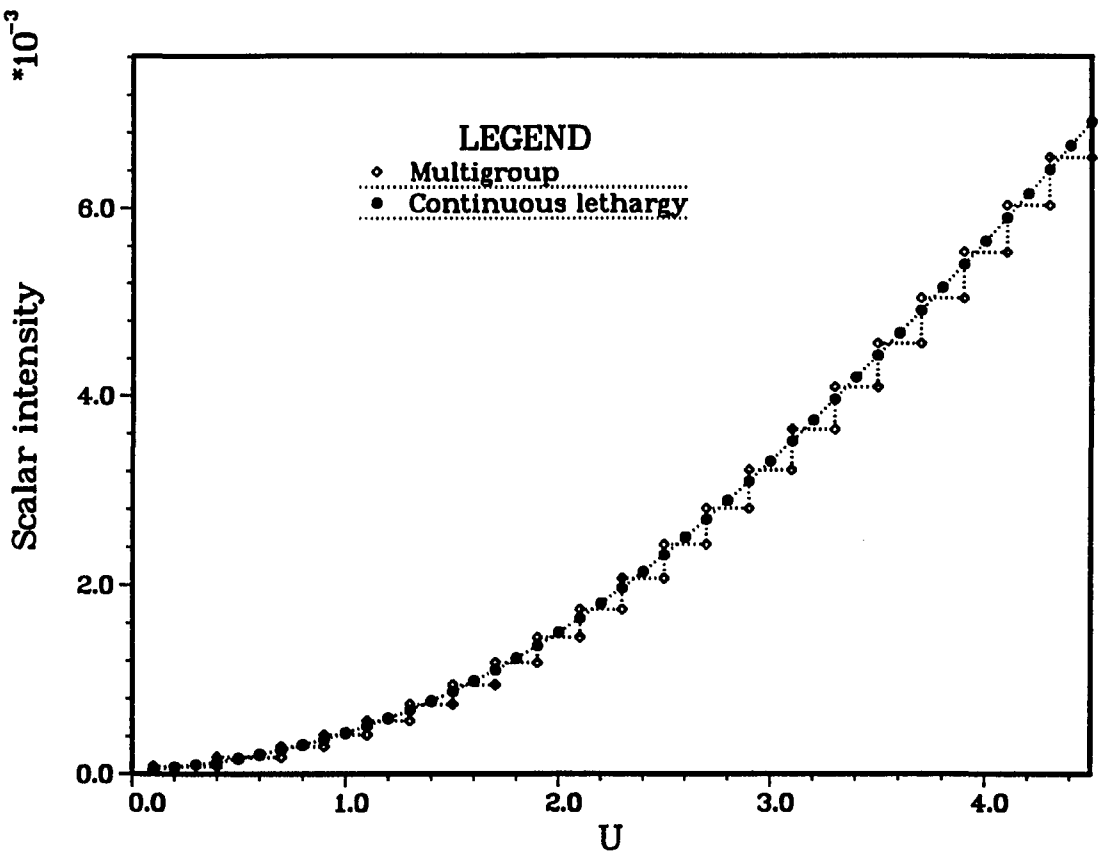

Figure 4.2k Comparison of Twenty-Three Group and Continuous Lethargy Results, t=10 at x=1

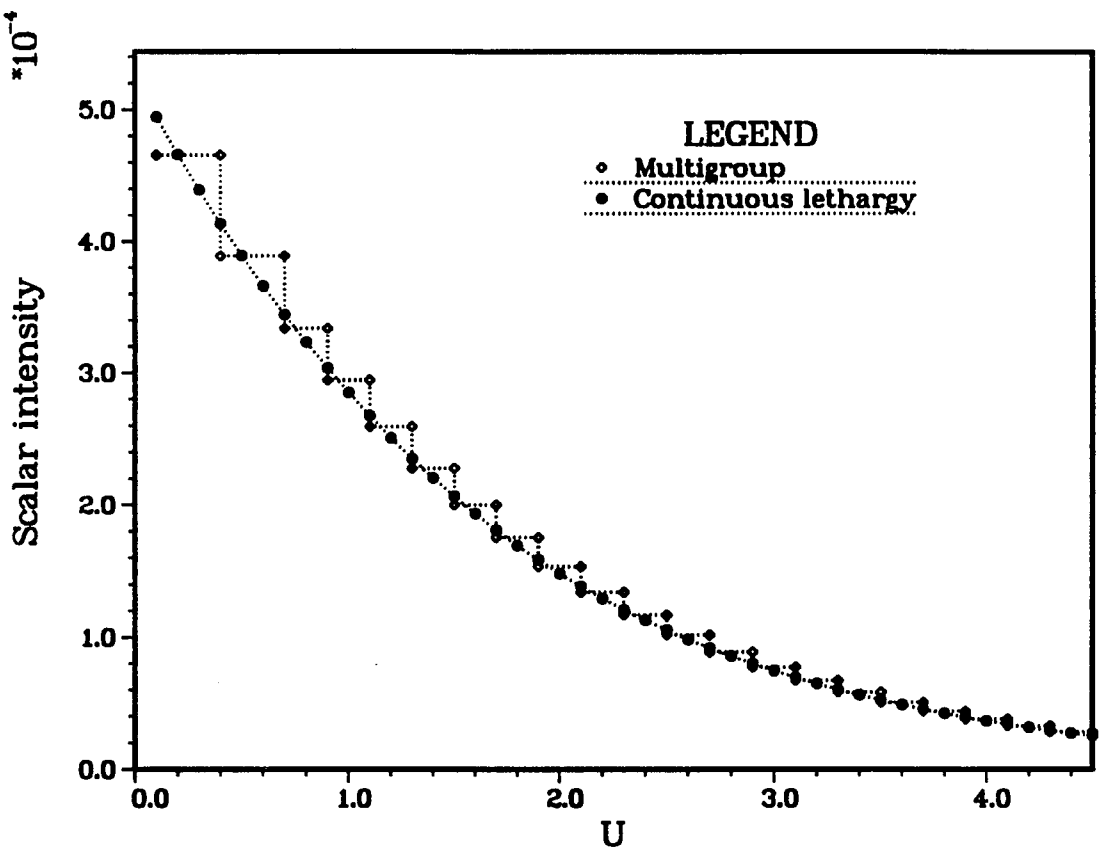

Figure 4.21 Comparison of Twenty-Three Group and Continuous Lethargy Results, t=5.2 at x=5

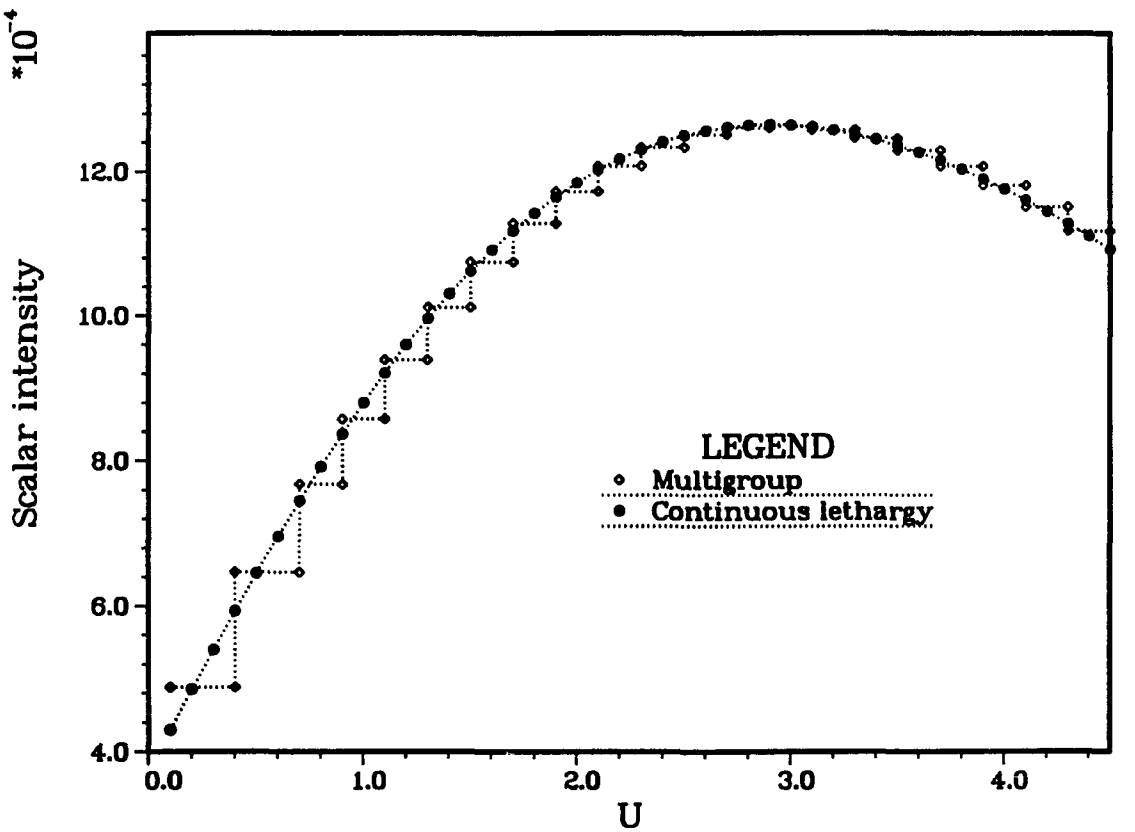

Figure 4.2m Comparison of Twenty-Three Group and Continuous Lethargy Results, t=7 at x=5

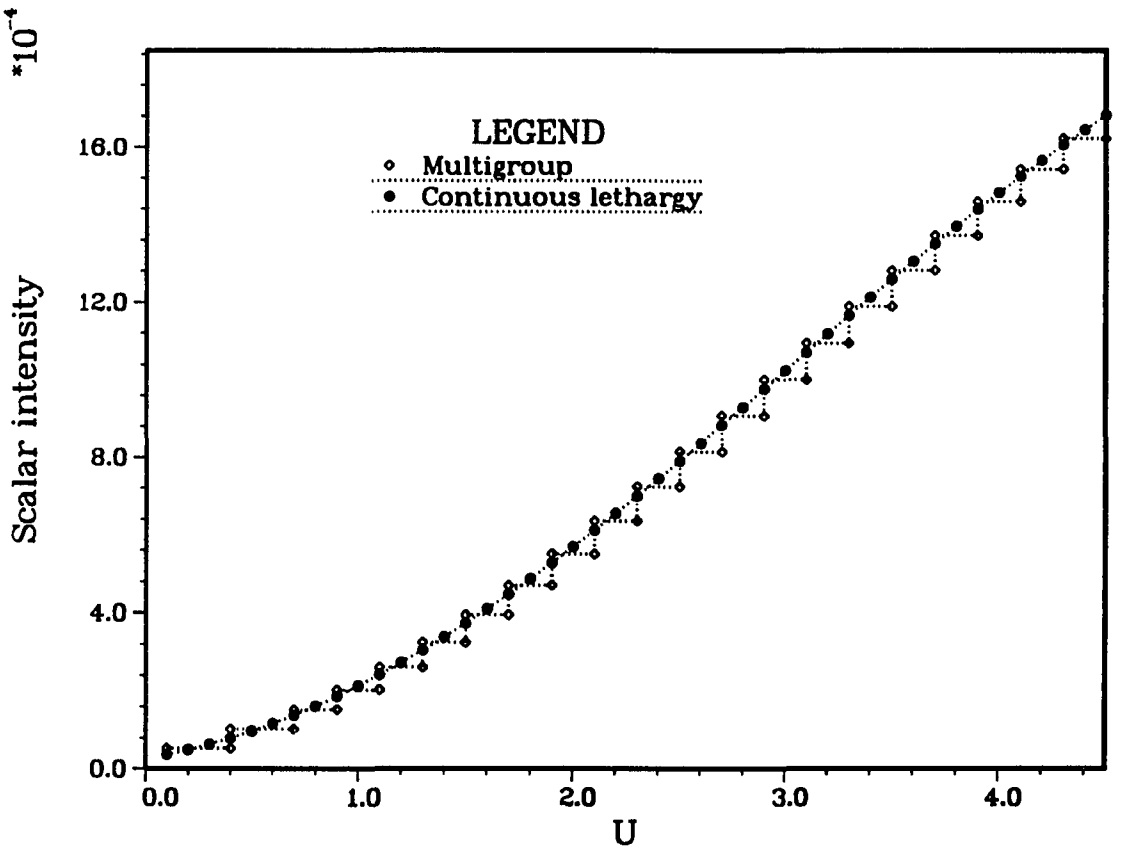

Figure 4.2n Comparison of Twenty-Three Group and Continuous Lethargy Results, t=10 at x=5

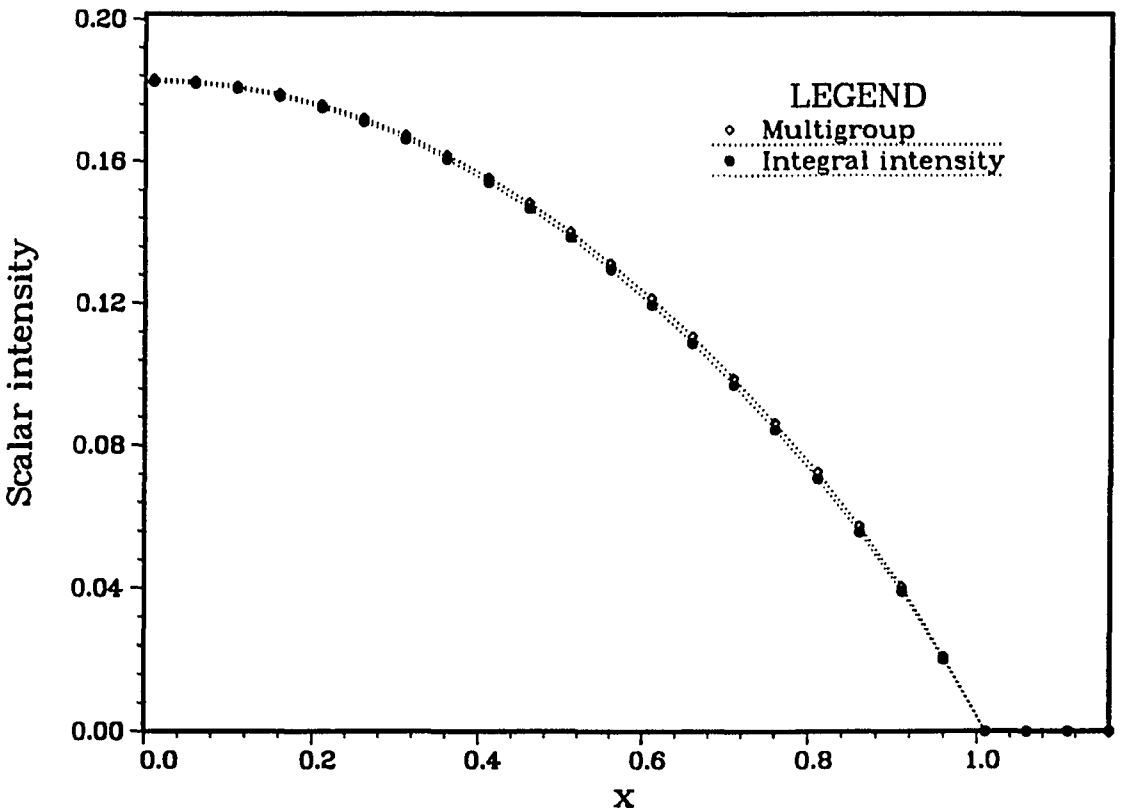

Figure 4.3a Comparison of Multigroup and the Integral of Continuous Lethargy Scalar Intensity in Group u=[0.1 1] at t=1

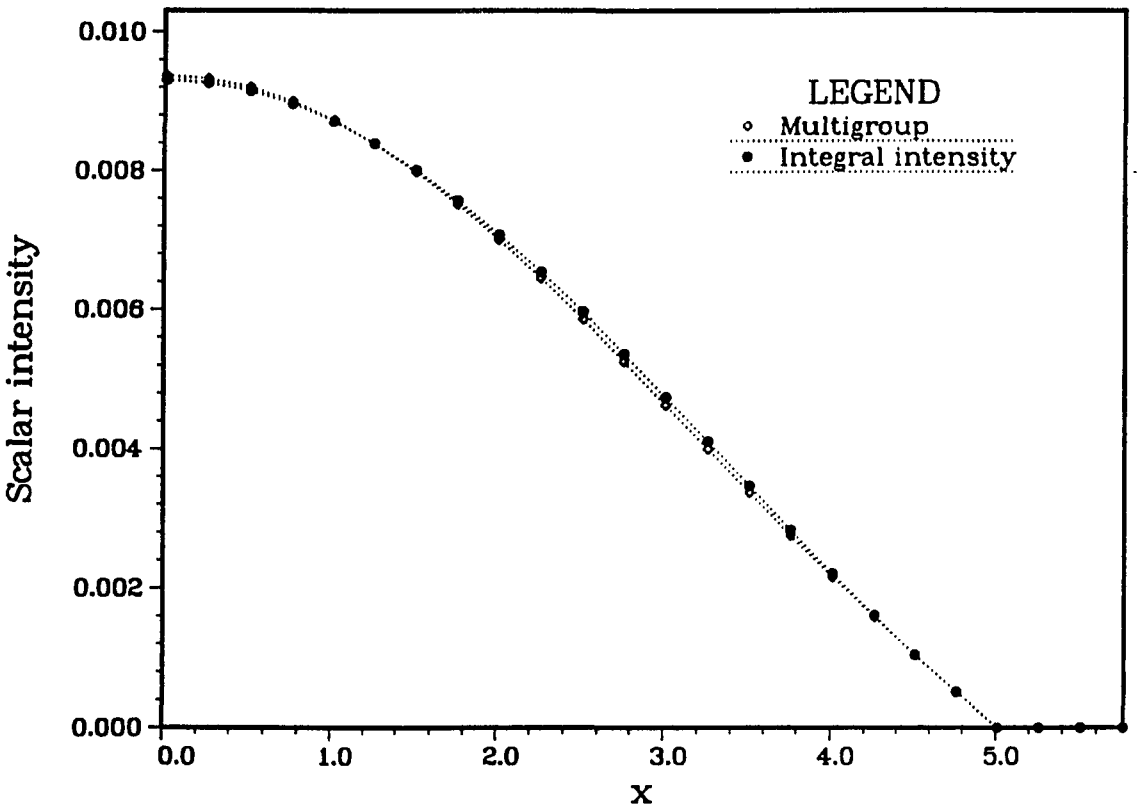

Figure 4.3b Comparison of Multigroup and the Integral of Continuous Lethargy Scalar Intensity in Group u=[0.1 1] at t=5

CHAPTER 5.
SUMMARY AND SUGGESTIONS

The subject matter of this thesis was divided into two major sections. In the first and most important section an analytical solution for the continuous lethargy time-dependent Boltzmann equation was generated. This solution was then applied to a fictitious radiative transfer problem demonstrating its benchmarking capability. In the second section a multigroup approximation for the same fictitious radiative transfer problem was compared to the benchmark solution in order to assess its accuaracy.

In the benchmark generation section, a fictitious radiative transfer problem was considered. The basis of the problem was Compton scattering, photon collisions with electrons at rest with the scattering kernel was assumed isotropic and dependent only on the lethargy differences before and after collisions. The constant speed of the photons provided the possibility of applying the Laplace transform in lethargy reducing the problem to a one-group problem. After Laplace transforming the lethargy variable as well, the resulting equation was then attacked by the multiple collision formulation method. Finally, the equation was formally solved giving a non-transparant (with Laplace inversion of lethargy remaining) analytical representation. The analytical representation was then evaluated to obtain a solution suitable as a numerical benchmark. For simplicity the Laplace transform

inversion of $\bar{f}(p)^n$ for the particular scattering kernel $f(u-u') = e^{-\alpha(u-u')}\theta(u-u')$ was evaluated analytically. The main effort of this research was the numerical evaluation of the analytical representation given by equation (2.18). Since no discrete approximations were made in deriving the analytical solution, very accurate results were obtained for use as a standard in testing the validity of numerical transport algorithms or as an approximation to real situations. For a purely scattering medium, and $\alpha < 1$ in the scattering kernel of the system was found to be reproductive similar to to the supercritical neutron case. Some graphical representations were then given illustrating the time-dependent nature of the problem.

In the second section, the physically interesting multigroup approximation to the continuous lethargy equation was studied. The photon intensity was treated collectively. The multigroup radiative transfer equation was derived from the continuous lethargy equation by discretion of the lethargy variable. The resulting multigroup equations were then solved by the multiple collision formulation. No spatial or time discretization was applied to the resulting multigroup equations. Instead, the time and position variables were treated continuously, making the multigroup results accurate and also reliable. A five group calculation was first performed and compared to an already existing time-dependent one-group benchmark. The results of this comparison indicated that the multigroup algorithm was correct. Finally, after the validity of multigroup algorithm was verified, ten group and twenty-three group calculation were performed for comparison to the continuous lethargy benchmark solution. The results of this comparison were also presented and excellent agreement was obtained. That indicated that the multigroup algorithm is accurate.

The techniques developed here are very powerful and provide excellent results for those interested in benchmarks. Although not contained in this work, the method is extendable to to the higher-order anisotropic scattering, and nongray media. By means of the plane-point and point-line transformations, this approach may also be directly applied to infinite spherical and cylindrical geometries. Furture work could also include cross sections with a polynomial time dependence.

REFERENCES

1. C. E. Siewert and P. F. Zweifel, *Ann. Phys.* (N.Y.) 36,61,1966
2. K. M. Case, *Ann. Phys.* (N.Y.) 9,1 (1960).
3. K. M. Case and P. F. Zweifel, *Linear Transport Theory*, Addison-Wesley, Reading(1967).
4. N. Papmehl, *Nucl. Sci. Eng.* 28, 190(1967)
5. V. C. Boffi, *Nukleonik* 8, 448 (1966).
6. J. Palmeri, *TTSP* 16(7),1987
7. J. Palmeri, Exact Solutions to the Time-dependent Lorentz Gas Boltzmann Equation: The Approach to Hydrodynamics, Loomis Laboratory Report, 1989
8. B. D. Ganapol, *J. Comp. Phys.*, 59,768(1985)
9. B. Ganapol and L. Grossman, *Nucl. Sci. Eng.* 52, 454(1973).
10. B. Ganapol, P. McKenty, and K. Peddicord, *Nucl. Sci. Eng.* 64,317(1977).
11. B. Ganapol, *Nucl. Sci. Eng.* 92, 272(1986).
12. B. Ganapol, *TTSP*, 9(4), 145-159(1980).
13. J. R. Lamarsh, *Nuclear Reactor Theory*, Addison-Wesley, NY, 1972.
14. B. Ganapol, *International Topical Meeting on Advances in Reactor Physics*, Mathematics and Computation, Vol. 3, 1345-1351(1987).

15. G. Pomraning, Los Alamos Lecture Notes, 1986

16. F. P. Incropera and D. P. Dewitt, *Introduction to Heat Transfer*, John Wiley and Sons, Inc. (1985)